Atmos. Meas. Tech. Discuss., https://doi.org/10.5194/amt-2017-419
Manuscript under review for journal Atmos. Meas. Tech.
Discussion started: 2 January 2018

Atmospheric Measurement Techniques Discussions

Characterization of a catalyst-based total nitrogen and carbon conversion technique to calibrate particle mass measurement instrumentation

Chelsea E. Stockwell[1,2], Agnieszka Kupc[1,2], Bartlomiej Witkowski[1,2,3], Ranajit K. Talukdar[1,2], Yong Liu[4], Vanessa Selimovic[5], Kyle J. Zarzana[1,2], Kanako Sekimoto[1,2], Carsten Warneke[1,2], Rebecca A. Washenfelder[1], Robert J. Yokelson[5], Ann M. Middlebrook[1], James M. Roberts[1]

[1]NOAA Earth System Research Laboratory (ESRL), Chemical Sciences Division, Boulder, CO 80305, USA

[2]Cooperative Institute for Research in Environmental Sciences, University of Colorado, Boulder, CO 80309, USA

[3]University of Warsaw, Faculty of Chemistry, al. Żwirki i Wigury 101, 02-089, Warsaw, Poland

[4]University of Colorado Denver, Department of Chemistry, Denver, CO 80217, USA

[5]University of Montana, Department of Chemistry, Missoula, MT 59812, USA

Correspondence to: C. E. Stockwell (Chelsea.Stockwell@noaa.gov); J. M. Roberts (James.M.Roberts@noaa.gov)

Abstract. The chemical composition of aerosol particles is a key aspect in determining their impact on the environment. For example, nitrogen (N)-containing particles impact atmospheric chemistry, air quality, and ecological N-deposition. Instruments that measure total reactive nitrogen (N_r = all nitrogen compounds except for N_2 and N_2O) focus on gas-phase nitrogen and very few studies directly discuss the instrument capacity to measure the mass of N_r –containing particles. Here, we investigate the mass quantification of particle-bound nitrogen using a custom N_r system that involves total conversion to nitric oxide (NO) across platinum and molybdenum catalysts followed by NO-O_3 chemiluminescence detection. We evaluate the particle conversion of the N_r instrument by comparing to mass derived concentrations of size-selected and counted ammonium sulfate ($(NH_4)_2SO_4$), ammonium nitrate (NH_4NO_3), ammonium chloride (NH_4Cl), sodium nitrate ($NaNO_3$), and ammonium oxalate ($(NH_4)_2C_2O_4$) particles determined using instruments that measure particle number and size. These measurements demonstrate N_r-particle conversion across the N_r catalysts that is independent of particle size with 98 ± 10% efficiency for 100 – 600 nm particle diameters. We also show conversion of particle-phase organic carbon species to CO_2 across the instrument's platinum catalyst followed by a non-dispersive infrared (NDIR) CO_2 detector. We show the N_r system is an accurate particle mass measurement method and demonstrate its ability to calibrate particle mass measurement instrumentation using single component, laboratory generated, N_r-containing particles below 2.5 µm in size. In addition we show agreement with mass measurements of an independently calibrated on-line particle-into-liquid sampler directly coupled to the electrospray ionization source of a quadrupole mass spectrometer (PILS-ESI/MS) sampling in the negative ion mode. We obtain excellent correlations (R^2 = 0.99) of particle mass measured as N_r with PILS-ESI/MS measurements converted to the corresponding particle anion mass (e.g. nitrate, sulfate, and chloride). The N_r and PILS-ESI/MS are shown to agree to within ~6% for particle mass loadings up to120 µg m^{-3}. Consideration of all the sources of error in the PILS-ESI/MS technique yields an overall uncertainty of ± 20% for these single component particle streams. These

Atmos. Meas. Tech. Discuss., https://doi.org/10.5194/amt-2017-419
Manuscript under review for journal Atmos. Meas. Tech.
Discussion started: 2 January 2018

results demonstrate the N_r system is a reliable direct particle mass measurement technique that differs from other particle instrument calibration techniques that rely on knowledge of particle size, shape, density, and refractive index.

1 Introduction

Aerosol particles are a key component of the atmospheric chemical environment as they have climate, human health, and ecosystem effects (Pöschl, 2005; IPCC, 2013). Measuring aerosol particle chemical composition is a challenging endeavor that has been the subject of a great deal of innovation in the past few decades (Jayne et al., 2000; Weber et al., 2001). The calibration of these instruments has evolved to better detect speciated composition. Still, there is a need for fundamental mass-based calibration techniques to place aerosol particle measurements firmly in the context of other atmospheric chemical observations.

Nitrogen (N) compounds are major constituents of atmospheric aerosol and play a significant role in atmospheric chemistry, radiative balance, air quality, and N-deposition in both terrestrial and aquatic ecosystems (Neff et al., 2002; Liao et al., 2003; Forster et al., 2007; Cornell, 2010; Xu et al. 2012; Park et al., 2014; Fuzzi et al., 2015). The relative contribution of N-compounds, specifically particulate nitrate, to total atmospheric particle mass is expected to increase in the coming century due to a projected reduction in SO_2 and increasing NH_3 (Bauer et al., 2007; Bellouin et al., 2011; Hauglustaine et al., 2014; Li et al., 2015), and already dominates in some urban and agricultural environments (Haywood et al., 2008; Vieno et al., 2016). Excluding N-species in deposition studies contributes to uncertainty in regional and global nitrogen budgets used to evaluate ecological, biogeochemical, and climate impacts (Jickells et al., 2013; Cornell, 2010; Cape et al., 2011). Measuring individual N-species, classes of N-compounds, or total N is challenging, and laboratory and field data are limited. For example, while there are a number of methods to measure inorganic N species, particulate organic N is more difficult to quantify with fewer sampling and measurement methods currently available for such a variety of compounds (Lin et al., 2010; Farmer et al., 2010; Lee et al., 2016). Measuring the total N mass of atmospheric particles will improve our understanding of their role in nitrogen cycles associated with sources such as agriculture or wildfires, and processes such as photochemical oxidation.

Several techniques exist to measure total reactive nitrogen (N_r), defined here as all atmospheric nitrogen excluding N_2 and N_2O, which includes both gas (e.g. total odd nitrogen (NO_y), NH_3, amines, nitriles, nitrates, etc.) and particle phase species (e.g. inorganic and organic N compounds). An established, rapid-response, robust technique for measuring N_r involves thermal and catalytic conversion to nitric oxide (NO) with detection by O_3 chemiluminescence. The catalyst material, temperature, and sampling methods dictate the efficiency, time resolution, and speciation of measurements (Winer et al., 1974; Williams et al., 1998; Dunlea et al., 2007; Schwab et al., 2007; Benedict et al., 2017). The chemiluminescence detection technique has been used to measure NO_x ($NO + NO_2$; Parrish and Fehsenfeld, 2000), total gas-phase N_r (e.g. Hardy and Knarr, 1982; Horstman, 1982), individual reactive nitrogen components (e.g. NH_3; Breitenbach and Shelef, 1973; Saylor et al., 2010), or subsets of nitrogen compounds by removal of selected compounds using filters or denuders upstream (Prenni et al., 2014). Marx et al. (2012) completed the only study to explicitly report quantitative conversion of particle-bound N_r for a limited number of species, however the results show a range of conversion efficiencies (78 – 142%). Several other studies assume at least some (non-quantitative) particle conversion across their catalysts (Fahey et al., 1985, 1986; Prenni et al., 2014). To our

knowledge, no study selectively isolates particle-phase reactive nitrogen to assess the particle-phase contribution to total nitrogen signals from individual sources or in their atmospheric measurement. Here we characterize the particulate N_r conversion in our converter consisting of heated platinum and molybdenum catalysts followed by rapid chemiluminescence detection using common inorganic atmospheric N_r-species including $(NH_4)_2SO_4$, NH_4Cl, $NaNO_3$, NH_4NO_3, and $(NH_4)_2C_2O_4$. The application of the converter coupled with NO-O_3 chemiluminescence, hereafter referred to as the N_r system, to quantitatively convert and measure the sum of N_r particle mass was evaluated using mass concentrations determined using traditional particle instrument calibration methods.

Organic carbon species are major constituents of aerosol particles (Jimenez et al., 2009) and are responsible for some of the more important climate and health impacts of particles (Pöschl, 2005). Calibration of measurement systems for organic carbon species is a challenging task since there are thousands of possible compounds of differing sizes, functional groups and therefore volatilities (Jimenez et al., 2016; Murphy, 2016a, b). A comprehensive, mass-based technique for organic aerosol species would be a highly-desirable addition to the current measurement technology. Theoretically, the high-temperature platinum catalyst in our system should convert carbon species to carbon-dioxide (CO_2) in the presence of air. Conversion of volatile organic compounds (VOCs) to CO_2 on high temperature precious metal catalysts is a well-developed technique (see for example the Pt catalyst used in Veres et al., 2010). Total organic carbon measurements using similar catalysts (e.g. palladium/alumina) followed by reduction to methane have been used previously (Roberts et al., 1998; Maris et al., 2003). By these methods, Roberts et al. (1998) confirmed efficient conversion of C_1-C_7 gas-phase compounds across the catalyst. Platinum-based catalysts are widely used and have been shown to be more efficient than palladium in oxidation studies (Schwartz et al., 1971; Kamal et al., 2016). Here we characterize the conversion efficiency of particle-phase organic carbon across our Pt catalyst by direct measurements using a LICOR non-dispersive infrared (NDIR) CO_2 analyzer. The current converter specifications coupled with both NO and CO_2 detectors allows simultaneous measurements of N_r and total carbon (C_y).

Many traditional particle instrument calibration methods involve measurements of particle properties by inertial, gravitational, diffusional, electrical (e.g. sizing), thermal, or optical measurement devices (Chen et al., 2011). Generally, direct mass concentration calibration techniques involve off-line analysis of filters or semi-real time measurements (e.g. PILS combined with ion chromatography). More rapid techniques directly measure number concentrations and particle sizes. However, these methods often require knowledge of aerosol properties (e.g. composition, shape, density, refractive index) and sampling parameters (e.g. volumetric flow rate, pressure, temperature, relative humidity) in order to determine mass concentrations. While these instrument calibration techniques are well established for controlled laboratory generated aerosol standards, the N_r system is an alternative that directly measures mass traced back to gas phase calibration standards instead of relying on particle size, shape, or refractive index.

In order to demonstrate the application of the N_r system to directly measure particle mass to calibrate particle mass measurement instrumentation, we compare mass concentrations measured by a new approach of directly coupling a particle-into-liquid sampler to the electrospray ionization source of a quadrupole mass spectrometer (PILS-ESI/MS) for on-line mass analysis of water-soluble aerosols. The Particle-into-Liquid Sampler (PILS) is an

established technique developed to efficiently collect the water-soluble fraction of aerosol (Weber et al. 2001; Orsini et al., 2003; Sorooshian et al., 2006). Here, we couple the PILS with an independently calibrated electrospray interface followed by mass detection to obtain on-line mass measurements of single-component, laboratory generated, N_r-containing aerosol that can be directly calibrated using the N_r system.

In this work, we present the converter set-up, system methodology, and evaluate the particle-conversion efficiency of a custom N_r system for several atmospherically relevant N_r-containing particles. The conversion efficiency of the N_r-catalyst was evaluated by comparing the N_r mass signal with the mass calculated from instrument calibration techniques that measure the particle number size distributions of laboratory-generated aerosols of known composition. We then show the quantitative conversion of organic carbon across the instrument's platinum catalyst followed by CO_2 detection. Finally we compare particle mass directly measured using a particle-into-liquid sampler coupled directly to an electrospray ionization source and by the N_r instrument. The primary objective of these experiments is to characterize particle conversion in the N_r system, and to investigate the capabilities of the N_r system as a calibration instrument that directly measures particle mass concentration.

2 Experimental details

2.1 Description of the total reactive nitrogen (N_r) system

Measurements of total reactive nitrogen, N_r, were accomplished by catalytic conversion to NO and detection of the NO using a chemiluminescence instrument. This NO-O_3 chemiluminescence instrument is a custom-built version of the common atmospheric monitoring instrument (Williams et al., 1998) and is calibrated directly with gas phase standards of NO. All the N_r species were converted to NO or NO_2 on a high temperature catalyst, and the NO_2 subsequently converted to NO on a lower temperature catalyst. The high-temperature catalyst system consisted of a quartz tube (13 mm OD x 11 mm ID x 35 cm L) packed with 36 platinum (Pt) screens (Shimadzu Part No. 630-00105) run at high temperature (750°C), shown in Fig. 1. The catalyst bed was confined to an 8 cm long section by dimples in the quartz tube, and that section was positioned so that the gas reaching it had been equilibrated to 750°C, as confirmed by a thermocouple probe. The flow through the catalyst was set to 1 standard L min^{-1} via a downstream flow controller. The Pt surface area was 126 cm^2 and the residence time was 0.1 s at 83.3 kPa and 750°C. Platinum catalysts of this kind are also known to oxidize NO to NO_2, which has been the source of problems with some previous systems that were designed to measure atmospheric ammonia (NH_3) (Schwab et al., 2007). In our system, the Pt catalyst is followed by a molybdenum oxide (MoOx) catalyst consisting of a solid molybdenum tube (4.2 mm ID x 32 cm L) operated at 450°C, to which an 8 standard cm^3 min^{-1} flow of pure hydrogen was added to create a stable molybdenum oxide surface. Run in this manner, the MoOx surface did not require periodic treatment at higher temperatures under reducing conditions as described by Williams et al. (1998). The NO chemiluminescence detection scheme used for laboratory calibrations had a fundamental sensitivity between 6 and 7 counts per parts per trillion (pptv) and the detection limit determined by the background signal in zero air was typically 0.15 pptv (4 σ) for a 1 s measurement. The operation of this instrument during these experiments often required considerable de-tuning to keep

Atmos. Meas. Tech. Discuss., https://doi.org/10.5194/amt-2017-419
Manuscript under review for journal Atmos. Meas. Tech.
Discussion started: 2 January 2018

the instrument count rates below the roll-over point of the photon counting electronics (approximately 5 MHz), thus the detection limit was closer to 0.1 ppbv for these measurements.

2.1.1 Nitrogen-containing particles

The measurement of particle phase N_r requires decomposition or volatilization of the solid material, followed by catalytic conversion to NO (or NO_2). Broadly, there are three types of N_r-containing particles, with a range of thermal stabilities from volatile to refractory. First, there is considerable literature that indicates that small particles composed of two major semi-volatile species, ammonium nitrate (NH_4NO_3) and ammonium chloride (NH_4Cl), will dissociate to constituents NH_3 and HNO_3 (and HCl), when modestly heated to temperatures < 100°C (Huffman et al., 2009; Hu et al., 2011). These materials will be readily converted on high temperature catalysts (e.g. platinum, Pt) as gas phase NH_3 and HNO_3. The second type of N_r-containing particles include intermediate stability compounds consisting mostly of nitro-organics (R-NO_2), organic nitrates ($RONO_2$), and amine and ammonium salts of acids. These compounds begin to decompose at relatively low temperatures. For example, thermal decomposition studies of bulk ammonium oxalate ($(NH_4)_2C_2O_4$) indicate that it begins to decompose at temperatures slightly above 200°C (Usherenko et al., 1998). Similarly, bulk samples of ammonium sulfate ($(NH_4)_2SO_4$) and ammonium bisulfate ($(NH_4)HSO_4$) decompose at approximately 150–250°C depending on water content (Kiyoura and Urano, 1970). Given sufficient residence time, intermediate volatility compounds will start to convert to gas-phase products in the hot inlet tubing and fully convert to NO (or NO_2) on a hot Pt surface (750°C). The third type of N_r-containing particles are composed of refractory salts such as sodium nitrate ($NaNO_3$), which will be the most resistant to decomposition and require contact with high temperature surfaces of the Pt catalyst. Studies of the thermal decomposition of $NaNO_3$ on Pt surfaces indicate that NO is evolved starting at about 500°C. In summary, the existing literature suggests that the thermal decomposition/conversion of N_r-containing particles to NO (NO_2) is thermodynamically feasible provided there is sufficient residence time and surface area in the catalyst zone.

2.2 Description of the PILS-ESI/MS

A schematic of the PILS-ESI/MS is shown in Fig. 2. The Particle-into-Liquid Sampler (PILS; Brechtel Manufacturing Inc., Hayward, CA) was developed by Weber et al. (2001) and collects water-soluble aerosol compounds by growing particles into liquid droplets in a supersaturated water environment and then collecting the droplets. A detailed description of the PILS used in these studies can be found in Sorooshian et al. (2006). The PILS is an established water-soluble aerosol collection technique that has been coupled with various mass analysis methods and was used previously by other laboratories in instrument evaluation studies (e.g. Drewnick et al., 2003; Takegawa et al., 2005; Canagaratna et al., 2007).

The PILS sample flow was set to 100 µL min^{-1} and was continuously mixed with an acetonitrile flow (100 µL min^{-1}). The 1:1 volume mixture of acetonitrile and water was directed toward the custom electrospray ionization source (at ~10 µL min^{-1}) of a commercial quadrupole mass spectrometer (Balzers Instruments, QMG 422)operated in negative ion mode for on-line analysis of selected water-soluble organic and inorganic compounds. The electrospray interface involved sample injection at ambient pressure through a fused silica capillary tip (30 µM ID) with a 2.5 L

min^{-1} N_2 sheath flow at a spray voltage of -3.5 kV. The MS instrument was modified from the negative-ion proton-transfer chemical-ionization mass spectrometer (NI-PT-CIMS) described in Veres et al. (2008). The flow tube was replaced with a stainless steel capillary inlet connected to the front region (I; shown in Fig. 2) held at ~300 Pa. Ions were focused across this region using a planar DC ion carpet (Anthony et al., 2014) mounted in front of the orifice leading to the second region (II). The ions were then accelerated through the collisional dissociation chamber (CDC) and collimated in the octopole ion guide at a total pressure of ~1 Pa (region II). The ions were transferred to the quadrupole mass spectrometer (region III). The electron multiplier detector was maintained at a pressure of less than 6.6×10^{-3} Pa.

The ESI/MS was calibrated using volumetrically and gravimetrically prepared liquid-phase standards of the anions associated with the target compounds (e.g. SO_4^{2-}, NO_3^-, Cl^-) (Sigma Aldrich, St. Louis, MO). Anion-specific calibration factors were calculated from linear least-squared fits of multi-point calibration curves. The uncertainty in the slope resulted in a maximum uncertainty of ~10% for the compounds tested. The ESI flow rate, solvent composition, analyte chemical properties, and matrix effects potentially impact the ionization and transmission efficiencies of compounds (Kostiainen and Kauppila, 2009). For these reasons, experiments were performed under similar, or as close to identical, conditions as the calibrations for instrument evaluation. For purposes of this comparison, matrix effects were assumed to be negligible for tests sampling single-component aerosols. The limits of detection for the anions measured with the PILS-ESI/MS were below ~0.1 µg m^{-3} for the current system and sampling conditions. Sorooshian et al. (2006) discuss volatility losses in the PILS for several inorganic species and reported negligible loss with a collection efficiency of ≥96% for mass loadings of Cl^-, SO_4^{2-}, and NO_3^- ranging from 1-140 µg m^{-3}. Additionally, Orsini et al. (2003) showed the collection efficiency of ≥95% for particles as small as 30 nm diameter for a 15 L min^{-1} sample flow rate. Ammonium (NH_4^+) is the major ion susceptible to volatilization as shown in Ma (2004), who indicated an underestimation of ~15%. In this study, because we were operating in the negative-ion mode, we did not measure NH_4^+ directly.

2.3 Particle generation, measurement, and characterization

Several aerosols were generated including polystyrene latex spheres (PSL; Nanosphere size standards, Thermo Fisher Scientific Inc., Waltham, MA), NH_4NO_3, $(NH_4)_2SO_4$, $(NH_4)_2C_2O_4$ (Sigma Aldrich, St. Louis, MO), NH_4Cl (J.T. Baker Chemical Co., Phillipsburg, NJ), and $NaNO_3$ (Fisher Scientific, Hampton, NH). Aerosol particles were generated by atomization of aqueous solutions of pure compounds in distilled water (~0.5– 6 g L^{-1}) using a custom-built Collison-type atomizer (Liu and Lee, 1975) in a dry particle-free nitrogen flow. The output flow was dried using a silica gel diffusion dryer to a relative humidity less than 10%. The dry polydisperse particles were then size-selected using a custom-built differential mobility analyzer (DMA; Knutson and Whitby, 1975). The DMA was operated at a sample flow of 0.3–0.5 volumetric L min^{-1} and a ratio of 10:1 between the sheath and sample flow. The monodisperse particles were diluted with ultra-high purity filtered zero air (range 1–10 L min^{-1}) before entering a mixing vessel. In instances where a mixing vessel was not available, a segment of smaller diameter tubing was added in-line to promoted mixing prior to the flow being divided among the instruments. A condensation particle counter (CPC; 3022A, TSI Inc., Shoreview, MN) (Stolzenburg and McMurry, 1991) continuously measured the particle

number concentration of the output flow following dilution. We measured the flow pre- and post-sampling using a low-flow DryCal (Mesa Laboratories, Lakewood, CO) and estimate an uncertainty in the CPC flow rate calibration to be ± 1%. During several experiments, the aerosol flow was split and sampled by an ultra-high sensitivity aerosol spectrometer (UHSAS; Droplet Measurement Technologies, Longmont, CO) to continuously measure the particle concentration and size distribution for particles with diameters between ~63 and 1000 nm.

In these experiments particle diameters from 100 to 600 nm were selected and the multiply-charged particles in the size distribution were accounted for as described below. For the liquid concentrations and atomizer conditions we used, the DMA output size distribution is a multi-peaked population consisting not only of singly charged particles but also particles with multiple (mostly two or three) charges. The multiply charged particles can contribute significantly to the overall mass and must be considered when calculating particle mass. The distributions of singly, doubly, and triply charged particles can vary depending on the solution concentration. We measured atomized size distributions using the scanning mobility particle sizer (SMPS; Wang and Flagan, 1990) function of the DMA (physical diameter, D_p = 1-1000 nm). The DMA transfer theory (Knutson and Whitby, 1975; Stolzenburg, 1988) with Wiedensohler's (1988) steady-state charge distribution approximation was used to estimate the fraction of multiply charged particles contributing to the CPC number concentration for each diameter setting. There are a number of possible sources of uncertainty using these methods that may include particle losses, DMA transfer function uncertainty, counting uncertainty, and inversion errors. Consequently, the size distribution of particles selected at a particular voltage and flow setting of the DMA was examined using the UHSAS. UHSAS particle sizing is a function of the amount of light scattered onto the photodetectors. The quantity of scattered light, however, depends not only on the particle size, but also on the composition-dependent particle refractive index (Bohren and Huffman, 1983; Liu and Daum, 2000; Hand and Kreidenweis 2002; Rosenberg et al., 2012). The UHSAS manufacturer recommended calibration uses PSL microspheres, which are well characterized and have known refractive index (n = 1.58) and shape. Because the UHSAS sizing is sensitive to particle refractive index, a new sizing calibration curve was produced for each studied particle type (i.e. refractive index) (Kupc et al., 2017). Considering this, we used the DMA, with sizing accuracy ~ ± 2.5% and NIST-traceable PSLs for 150 –500 nm spheres as our calibration standard. The UHSAS sizing was recalibrated by using the DMA to select particles of known size for each of the aerosol types studied. A different UHSAS calibration curve was produced and used for each aerosol type (e.g. Kupc et al., 2017). These calibration curves were used to retrieve accurate particle size distributions so that the multiply charged particles were properly accounted for.

Previous laboratory studies show UHSAS and CPC number concentration comparisons in excellent agreement (Cai et al., 2008; Kupc et al., 2017), however, occasionally only a ~90% counting efficiency for the UHSAS was observed when compared to the CPC. These differences are attributed to particle coincidence at high concentrations (> 1000 cm^{-3}), and to inefficient particle mixing before reaching the instruments. Corrections for particle coincidence were applied (Kupc et al., 2017) though we expect differences due to particle mixing adds an additional 10% uncertainty to the measurements. For these reasons, we used the UHSAS size distributions to estimate the fraction of singly, doubly, and triply charged particles together with the total particle number taken from the CPC measurement to exclusive particle mass from total volume and density. The UHSAS and CPC measured particle

number concentrations were generally within 10% of each other, however, the CPC values did not require coincidence corrections and had a better signal to noise ratio.

3 Results and discussion

3.1 Characterization of the N_r system

3.1.1 N_r gas-phase conversion efficiency

We verified the efficiency of conversion of a range of gas phase N_r compounds in this catalyst system using calibrated gas mixtures or standard streams and auxiliary analysis methods. We compared the total N_r signal measured as NO, where NO was calibrated using NO standards in nitrogen (Scott-Marrin Inc., Riverside, CA) to the known amount specified by the calibration method. The conversion efficiencies are summarized in Table 1 and range from 95% to 110%. The values were based on the ratios of the N_r measured as NO to the expected values specified by each calibration method. The uncertainties in the measured conversion efficiencies encompass the propagated errors in each calibration method. For example, the largest uncertainty in the NH_3 conversion efficiency was the NH_3 UV absorption cross section at 184.9 nm (value of $4.4 \pm 0.3 \times 10^{-18}$ cm^2 taken from Neuman et al., 2003). It is possible that there were N_r compounds in the standard stream aside from NH_3 that were responsible for the result being >100%. However, the fact that the determination was above 100% for both a permeation source and a gas-phase mixture (3.1 ppmv in N_2) implies that the UV absorption cross section is high by 5-10% or that there were contaminants in both calibration sources. NH_3 is one of the more important reactive nitrogen species in the atmosphere-biosphere system and is thermodynamically one of the more difficult to convert. Compounds considered NO_y species, such as nitric acid, acetyl peroxynitrates, and alkyl nitrates were not studied in this work (aside from NO_2), since they are known to be converted at high efficiency on precious metal (Fahey et al., 1986) or molybdenum oxide (Winer et al., 1974) catalysts. The resulting uncertainties in the N_r measurement are estimated to be ± 10% based on comparisons of measured NO signals to individual N_r compound calibrations.

The conversion of nitrous oxide (N_2O) is a potential interference in the N_r method as N_2O is not typically considered a reactive nitrogen compound in the troposphere. Several experiments were conducted to determine the extent of this potential interference using a 10.1 ppmv N_2O standard. The resulting conversion efficiency ranged from 0.03% to 0.05% in dry and humidified air respectively. These can be considered upper limits for this interference as we cannot be completely sure that there were no N_r contaminants (e.g. NO_2) in the N_2O standard. This conversion efficiency upper limit is a negligible interference in the N_r measurements in ambient air or zero air matrices, and likewise will not be significant in biomass burning sources given that N_2O enhancements in fresh biomass smoke are generally not observed or contribute minimally to total nitrogen (Griffith et al., 1991). O_3 is another potential source of gas-phase interference due to the decomposition of O_3 to O_2 + O, followed by reaction of O with N_2O at high temperature to form NO. However, the NO production in the O + N_2O reaction is an approximately 20% channel with a net rate constant of approximately 1×10^{-15} cm^3 $molecule^{-1}$ s^{-1} at 750°C (NIST 2017). If all the O atoms from 70 ppbv of O_3 were available for reaction with an ambient level of N_2O (340 ppbv), then the 0.1 sec residence time in the

convertor would result in approximately 28 pptv of NO, an upper limit that is clearly a negligible amount in almost any atmospheric context.

3.1.2 N_r system set-up and response

The atomizer output was diluted with particle-free nitrogen and ultra-pure zero air, therefore, the N_r measurement should theoretically be attributed to particles only since no detectable gas-phase nitrogen is added to the sample stream. However, equilibration within the sample lines may result in outgassing and formation of gas-phase compounds affecting total N_r detection. Fig. 3(a) shows the initial response of the N_r system in cleaned inlets for $NaNO_3$. The N_r mass signal tracks the CPC-derived aerosol mass features closely as the aerosol source concentrations fluctuate. Additionally, as different particle sizes are selected by the DMA for $(NH_4)_2SO_4$ (Fig. 3(b)), changes in the total N_r response is fast and precisely tracks the changes in the CPC signal. The potential gas-phase constituents equilibrating in the lines from aerosols in this study include HNO_3, HCl, and NH_3. If these compounds formed before reaching the N_r catalyst it is likely adsorption and desorption from inlets and tubing surfaces would occur (e.g. Neuman et al., 1999; Yokelson et al., 2003). As an example, the presence of NH_3 in Fig. 3(b) (or HNO_3 in nitrate containing particles) would be indicated by a delayed and lengthened rise/fall in the N_r response with sudden changes to the input concentrations. However, the total N_r response precisely tracks the CPC signal suggesting that gas-phase NH_3 was not present in significant quantities. In experiments at exceptionally high aerosol loading of $(NH_4)_2C_2O_4$ (up to several ppmv of total N_r, i.e., several thousand µg m^{-3}) N_r signal "tailing" was observed suggesting that NH_3 was scavenging to the walls of the inlet before the heated quartz tubing.

Marx et al. (2012) reported calculated conversion efficiencies in air sampled from a small chamber for $NaNO_3$, NH_4NO_3, and $(NH_4)_2SO_4$ to be 78, 142, and 91%, respectively. The authors suggested the overestimation of NH_4NO_3 was a result of its semi-volatile properties under ambient conditions that led to the formation of gaseous NH_3 and HNO_3 in the chamber. For these reasons, we limit the background artifacts and volatilization effects that may have occurred during chamber filling and sampling in Marx et al. (2012) by sampling immediately following solution atomization through conductive tubing at relatively high sample flow rates. Additionally, we use a DMA to size-select the atomized polydisperse aerosol to evaluate the particle conversion efficiency at several different diameters (100 – 600 nm in 50 nm increments) to investigate the volatilization effects and conversion efficiencies of smaller particles for the extended list of N_r-containing aerosols studied in our work.

3.1.3 N_r-particle conversion efficiency

The voltage scanning (SMPS) function of the DMA and number concentration measurements by the CPC is a conventional method to determine particle size distributions, and for calculating particle mass from total volume and density, assuming spherical particles. For the total nitrogen measurements, the total particle-bound N_r mixing ratios were retrieved and converted to mass concentrations for each corresponding salt. Figures 4(a-d) show the calculated vs measured mass concentrations (µg m^{-3}) for particles of different composition and diameter. The plots show that a strong correlation ($R^2 > 0.98$) and good agreement was obtained for smaller particles (50 – 200 nm) with slopes ranging

from 0.86 – 0.97, while for larger particles (≥250 nm) the mass calculated values were sometimes as much as >50% too high. The R^2 for all particles including ≥ 250 nm ranged from 0.71 – 0.85 with slopes of 1.08 – 1.36.

For larger particles, we used a UHSAS to determine the size distribution of multiply-charged species exiting the DMA. The SMPS inversion-derived size distributions were generally broader than the UHSAS size distributions, though agreement improved at increased scan times. Small differences in the size distribution recovered from the voltage scans at larger diameters (> 200 nm) affected the mass distribution considerably because particle mass scales with diameter cubed. A possible explanation is that we are not correctly accounting for the delay time from the DMA exit to the CPC, therefore the particle counts did not correspond to the correct size designated from voltage scanning and this likely skewed the size distribution relative to the true distribution (Collins et al., 2002). Methods for limiting these effects exist (Russell et al., 1995; Collins et al., 2002) including slower voltage scan rates. However, our results demonstrate the added challenges in particle mass determination using estimated size distributions from the SMPS method. Other aerosol measurement techniques (e.g. the Particle Time of Flight mode of the Aerosol Mass Spectrometer; DeCarlo et al., 2006) directly measure size distributions or instead measure polydisperse aerosol and the instrument and inversion-algorithm corrections required using the SMPS are avoided. Therefore, we instead measure the size distributions directly using the UHSAS with particle concentration measurements (by either the CPC or UHSAS) to evaluate the N_r particle conversion in the N_r system.

For the aerosol mass concentrations (μg m^{-3}) calculated using UHSAS particle size distributions, we refer to these values as UHSAS calculated mass. Comparisons of the mass directly measured as N_r versus UHSAS calculated mass concentrations for atomized solutions of $NaNO_3$, $(NH_4)_2SO_4$, NH_4Cl, and $(NH_4)_2C_2O_4$ are shown in Fig. 5 with orthogonal distance regression lines with slopes that range from 0.910 – 1.06 for concentrations from ~0–70 μg m^{-3}. The instruments are highly correlated (R^2 = 0.90 – 0.99) and the fits indicate that for the salts tested there is quantitative conversion of particulate nitrogen, to within the combined uncertainties of the methods, independent of diameter (range: 100 – 600 nm). More detailed particle conversion efficiencies by size are shown in Table 2 for each aerosol tested. On average across all size ranges the results indicate 97 ± 7%, 101 ± 5%; 100 ±10%, and 93 ± 5 % particle conversion efficiencies for $NaNO_3$, $(NH_4)_2SO_4$, NH_4Cl, and $(NH_4)_2C_2O_4$, respectively. The largest deviation from the one-to-one line occurred for $(NH_4)_2C_2O_4$, which may imply some ammonia loss, though the agreement is generally still within 10% for most particle sizes.

For the case of NH_4NO_3, the UHSAS measured size distribution peaked at significantly lower diameters than expected based on the DMA size selection. This difference has been reported previously (Cai et al., 2008; Womack et al., 2017), though to a lesser extent (~8%) than observed here (up to 30%). Possible explanations for these differences could include vaporization/evaporation effects, residual water in the particles, surface effects, or differences in electrical mobility diameter and geometric diameter due to non-sphericity as discussed in DeCarlo et al. (2004). For these reasons, we made no attempt to characterize NH_4NO_3 behavior in either the DMA or UHSAS and refer to Sect. 3.2 for mass concentration comparisons of polydisperse aerosol measured using separate mass measurement techniques (both the N_r system and PILS-ESI/MS). It is worth noting that NH_4NO_3 is one of the more volatile compounds included in this study and it is reasonable to expect similar particle conversion efficiencies in the N_r system catalysts for NH_4NO_3 as the other species tested (Table 2).

Atmos. Meas. Tech. Discuss., https://doi.org/10.5194/amt-2017-419
Manuscript under review for journal Atmos. Meas. Tech.
Discussion started: 2 January 2018

3.1.4 N_r measurements of biomass burning

As an example of both gas and particle measurements using the N_r system, we follow with a brief discussion of N emissions from biomass burning. The primary gaseous N-compounds in biomass burning plumes include NO, NO_2, N_2, NH_3 and to a lesser extent HCN, CH_3CN, HONO, HNCO (Lobert et al., 1990; Lobert et al., 1991; Kuhlbusch et al., 1991; McMeeking et al., 2009; Burling et al., 2010; Stockwell et al., 2014; 2015) and other N_r-containing gases. Figure 6 shows results obtained from a representative fire (Fire 047) from the Fire Influence on Regional and Global environments Experiment (FIREX) 2016 Missoula Fire Lab study (https://www.esrl.noaa.gov/csd/projects/firex/). Figure 6(a) shows the co-measured N_r and NO concentrations (ppmv). The majority of the N_r system's response is due to the sum of gas-phase N_r-constituents that were measured by a Fourier transform infrared spectrometer (FTIR; Selimovic et al., 2017), an H_3O^+ chemical ionization mass spectrometer (Koss et al., 2017), and a broadband cavity enhanced extinction spectrometer (Min et al., 2016) (Fig. 6(b)). At the beginning of the burn (pre 10:23 AM) the average relative percent difference between the total nitrogen signal and the sum of individually measured gas-phase compounds is ~16%, which is less than the combined error of the individual measurements. There is greater disagreement shown in Fig. 6(c) (difference is up to ~1 ppmv; up to ~50% relative percent difference) during other stages of the fire. We have shown in our laboratory experiments that there is quantitative N_r particle conversion across the N_r catalyst, therefore, it is likely that particulate ammonium contributes to the excess N_r signal measured during periods dominated by smoldering combustion, while particulate nitrate likely accounts for some N_r signal during the flaming dominated stages as shown in Fig. 6. By confirming particulate N_r-conversion in this system, it is possible that a total N budget can be reconstructed for additional laboratory fires measured during the FIREX laboratory study where individual particle phase N_r data are available.

3.1.5 Carbon conversion efficiency of Pt catalyst

The high-temperature platinum catalyst (Fig. 1) in the N_r instrument should quantitatively convert carbon containing species to carbon-dioxide (CO_2) in the presence of air. Gas-phase carbon conversion across similar precious metals has been studied extensively (see for example the Pt catalyst used in Veres et al., 2010). Therefore, adding a CO_2 analyzer to the configuration allows for simultaneous measurements of N_r and C_y.

For the following experiments, the total flow through the Pt catalyst was increased slightly (~1.5 sL min^{-1}) and was then split after the Pt and before the MoOx catalyst, with the smaller flow (0.5 sL min^{-1}) directed through the LICOR 6251 (LI-6251; Lincoln, NE) CO_2 analyzer, and the main flow directed through the MoOx catalyst and the NO-O_3 chemiluminescence detector. The LICOR instrument was internally referenced to scrubbed zero air. The conversion of compounds that contain both N and C atoms can then be measured simultaneously using the NO-O_3 chemiluminescence detector and LI-6251 detector in parallel. At ambient CO_2 levels, it is challenging to retrieve reliable measurements since the signal relative to the background abundance of CO_2 is small. The approach described here relies on using ultra-pure air for aerosol generation and carrier gas flow, therefore ambient air is eliminated. The LI-6251 was calibrated with sub-5 ppm CO_2 standards (Scott-Marin Inc., Riverside, CA) in ultra-pure air. Due to the

low signals levels and the uncertainty of the low concentration CO_2 standards, the overall accuracy of the CO_2 measurements present in this work up to 1 ppmv is ± 10% for 10 second averages.

The efficient conversion of gas-phase C-compounds in our catalyst system was confirmed using a CO standard in air, and a combination CO_2, CO, CH_4 standard in air. The following discussion focuses on the conversion of particle-phase organic compounds (OC). The efficient conversion of N_r-containing particles was demonstrated in Sect. 3.1.3 for the range of N oxidation states. We are confident these results extend to other N_r-containing particles, which is supported by the extensive list of N_r gases efficiently converted as shown in Table 1. Therefore, we expect that the resulting N_r and C_y signals from each detector will be in proportion by dividing the result by the number of carbon and nitrogen atoms in the parent molecule to give the standard concentration on a molar basis. Polydisperse particulate OC was generated from solution following an N_2 purge to eliminate carbonate from the solution. Aerosol particles from solutions of anthranilic acid ($C_7H_7NO_2$, 2-aminobenzoic acid, Sigma Aldrich), threonine ($C_4H_9NO_3$, 2-amino-3-hydroxybutanoic acid, Sigma Aldrich), tryptophan ($C_{11}H_{12}N_2O_2$, 2-amino-3-indolylpropanoic acid, Sigma Aldrich), and quinine ($C_{20}H_{24}N_2O_2$, Sigma Aldrich) were tested. These compounds were chosen based on their water solubility to avoid the use of organic solvents. An example of the N_r and C_y response is shown in Fig. 7 for threonine (see Fig. S1 for additional compounds). The relative difference between the N_r and C_y measured concentrations (up to several hundred ppbv) is less than 10%, which is within the propagated uncertainties of the CO_2 calibration standards and both detection methods.

Initial tests with $(NH_4)_2C_2O_4$ proved more challenging as the low C number required large polydisperse aerosol loadings (several ppmv) to be measured reliably by the LICOR. During these instances, surface effects reduced the total N_r signal, which likely resulted from NH_3 scavenging to the walls of the transfer liens or quartz tubing. We conclude that the N_r system with a CO_2 detector in parallel can be used as a total carbon measurement system and would be useful to establish instrument calibrations for carbon-containing aerosol. The system is currently limited to calibration of compounds in zero air matrices because ambient levels of the common gas-phase carbon compounds CO_2, CO, and CH_4 are high.

3.2 Comparisons with the PILS-ESI/MS

3.2.1 N_r system as an aerosol mass measurement method

Here we demonstrate the capability of the total nitrogen system as an independent calibration method for aerosol measurement systems. N_r measurements of laboratory generated single-component inorganic and organic aerosol particles were used to characterize a novel configuration coupling a PILS with electrospray ionization interface followed by mass spectrometric detection. The strength of using the N_r system to calibrate the PILS-ESI/MS is that it is a direct method to calibrate the entire coupled on-line system. The current calibration approach involves liquid-phase standards to calibrate the ESI/MS independently from the PILS.

The inorganic salts selected for this study all contained N atoms, either in the cation, anion, or both. The total N_r measured as NO (in ppbv) included all the N atoms atomized from the single-component solution. Dividing the total N_r measurement by the number of N atoms in the parent molecule gives the standard concentration (in ppbv) of the corresponding anion (e.g. Cl^-, NO_3^-, SO_4^{2-},$C_2O_4^{2-}$). The mixing ratios (in ppbv) are converted to µg m^{-3} from the

Atmos. Meas. Tech. Discuss., https://doi.org/10.5194/amt-2017-419
Manuscript under review for journal Atmos. Meas. Tech.
Discussion started: 2 January 2018

molecular weight of the corresponding anion. We refer to these mass concentrations as "X measured as equivalent N_r" in the remainder of the text, where X is the corresponding anion of the aerosol particle. The anion mass calculated in this way was only necessary when comparing directly to PILS-ESI/MS measurements of nitrate, sulfate, chloride, and oxalate.

3.2.2 N_r and PILS-ESI/MS mass concentration comparisons

In coupling an aerosol collection technique (PILS) with an electrospray ionization source, water-soluble aerosol particles are speciated in real-time. To compare to the calibration approaches through liquid phase standards described in Sect 2.2 for the PILS-ESI/MS we performed particle mass comparisons using these methods with anion-specific mass concentrations derived from the N_r measurement system. A single-component aerosol was used to minimize complex matrix effects including ion suppression/enhancement common in ESI.

An example of the N_r system and PILS-ESI/MS co-sampling a laboratory generated polydisperse aerosol stream is shown in Fig. 8. Here we did not size-select aerosols, but measured all particle sizes below a 2.5 µm cut-off (URG cyclone, Chapel Hill, NC). There are two reasons for this experimental set-up: (1) Generating a sufficient aerosol mass concentration to calibrate the PILS-ES/MS was challenging because it requires a minimum flow of 11 L min^{-1}, while the DMA output flow is <1 L min^{-1}, therefore the DMA aerosol flow required a large dilution. Because a greater aerosol particle mass could be realized by directly sampling the polydisperse output of the atomizer, our analysis focuses on comparisons between N_r and PILS-ESI/MS without using the DMA size-selection. (2) Conventionally the PILS instrument samples with a cyclone with a 1 or 2.5 µm cutoff, which is similar to other mass measurement instruments including the aerosol mass spectrometer (AMS) and filter collection.

Figure 8 shows the aerosol nitrate (blue) trace from $NaNO_3$ particles measured by the PILS-ESI/MS shifted in time to account for the system delay time so that it aligns with the relatively steady concentration periods with the N_r trace (black). The PILS-ESI/MS had a response time of roughly 4-5 min in its current configuration. Several stages in the PILS system included mixing volumes (e.g. syringe pumps and mixing vessels) that prevented rapid response to rapidly changing concentrations and smeared the response. For instrument comparisons 60 s data were averaged and compared during periods with relatively steady concentrations (generally lasting 5- 10 min). Examples of PILS-ESI/MS traces aligned such that initial response of both instruments coincide are shown in Fig. S2.

The correlation plot of PILS-ESI/MS to equivalent anion mass measured as N_r for each aerosol-type ($NaNO_3$, $(NH_4)_2SO_4$, NH_4Cl, and NH_4NO_3) is shown in Fig. 9(a-d). The concentrations ranged from ~10–120 µg m^{-3} and the standard linear regression fits for each aerosol type are included in Fig. 9, and were highly correlated with a $R^2 = 0.99$. For $(NH_4)_2SO_4$, the concentration exceeded the linear dynamic range of the PILS-ESI/MS for sulfate (see Fig. S2(a); > 130 µg m^{-3}) as determined by liquid-standard calibration curves. The linear range of ESI is limited at high concentrations due to limited surface sites available for ionization (Tang et al., 2004). For this reason values outside the linear dynamic range of the PILS-ESI/MS (> 130 µg m^{-3}) for sulfate were excluded from the linear regression fit. NH_4NO_3 shows a similar, less pronounced trend, however, it is still included in the regression plot as it was difficult to isolate whether this was analyte suppression during electrospray ionization or a linear dynamic range issue. Based on the regression fits in Fig. 9, the difference between the PILS-ESI/MS and N_r system for each inorganic component

is less than 6%. The uncertainty in the ESI signal varies by compound and averaging time, however from the tests described here the maximum uncertainty is estimated ~15%. Combining this uncertainty with the uncertainty in the ESI calibrations (maximum ± 10%), the air and liquid flow rate (both ~± 4%), and dilution (~± 5%) in quadrature gives a total maximum uncertainty associated with mass measurements of ± 20%. So while the slope of the correlations of the two instruments (based on 60 s averages during periods with constant concentrations) shows a relative difference of less than ~6%, the uncertainty in the PILS/ESI measurement of single component aerosols is closer to ~ 20% and could be greater if the transmission and ionization efficiencies of the ESI differ from the efficiencies present during calibration periods. This uncertainty is greater than the uncertainty (± 10 %) reported for the PILS-IC instrument for ionic species in Weber et al. (2001) but lower than the AMS uncertainty for nitrate (33 %) and sulfate (35%) estimated by Bahreini et al. (2009), though the AMS has a much faster time response.

Even though greater aerosol particle mass could be produced by directly sampling the polydisperse output of the atomizer, our analysis also included measurements using the DMA size-selected output. During these tests the flow was divided between the N_r system, CPC, UHSAS, and PILS-ESI/MS with a large dilution flow that resulted in turbulent mixing (Re >4000). The CPC and UHSAS particle number concentrations showed improved agreement with turbulent mixing compared to earlier differences up to 10% at high concentrations discussed in Sect. 2.3 and were within a few percent of each other. Examples of the real-time temporal profiles for these measurements are shown in Fig. 10(a-d) with the PILS-ESI/MS time offset by several minutes to account for its delayed response. The calculated and measured aerosol mass time traces in Fig. 10 show agreement for all measurement techniques tested in this study. The figures indicate that the PILS-ESI/MS was not given sufficient time to rise to a steady constant concentration for the first diameter selected. This is confirmed by Fig. 10(b) during which 200 nm particles were size selected twice in succession with the first selection lasting only ~2 min before flushing with water quickly followed by a longer period of sampling at the same diameter. The PILS-ESI/MS concentration during this longer sampling period does reach the expected concentration as indicated by the N_r (black) and CPC (blue) concentrations. The time-series of oxalate in Fig. 10(d) shows agreement for the equivalent N_r and PILS-ESI/MS measured mass indicating these same calibration methods are effective for organic compounds, although the UHSAS was not sampling during this experiment. We conclude that the PILS-ESI/MS quantitatively measures single component inorganic aerosol for a range of sizes, however, the low particle throughput hindered our ability to evaluate the quantitative abilities of the PILS-ESI/MS system for particles < 200 nm diameter.

These results establish the quantitative abilities of this novel configuration (PILS-ESI/MS) for sampling simple single-component laboratory generated aerosol. We evaluated this previously uncharacterized mass measurement technique using both traditional particle number size distribution measuring systems and the total N_r mass measurement system. We show experimentally that the N_r system can be used as a mass calibration method for pure N_r-containing polydisperse aerosol. Calibrating the ESI/MS using direct injection of liquid standards combined with mass concentrations collected by the PILS is a valid approach for quantifying inorganic components of aerosols, which likely extends to several organics as demonstrated by oxalate. However, these ESI/MS calibrations are sensitive to the experimental conditions, which must be precisely maintained during ESI calibrations and throughout the entire sampling period. Changes in flow rate, interface positioning, or solvent composition have significant impacts on both

Atmos. Meas. Tech. Discuss., https://doi.org/10.5194/amt-2017-419
Manuscript under review for journal Atmos. Meas. Tech.
Discussion started: 2 January 2018

Atmospheric Measurement Techniques Discussions

the transmission and ionization efficiency ultimately effecting pre-determined ESI calibration factors. Additionally, PILS characterization has been limited to theoretical predictions or experimental comparisons that involve coupling the PILS with a mass analyzer (e.g. IC; Orsini et al., 2003; Sorooshian et al., 2006). Here we introduced a new method for calibrating the entire PILS-ESI/MS coupled system using N_r equivalent mass measurements of Cl^-, NO_3^-, SO_4^{2-}, $C_2O_4^{2-}$ from N_r-containing particles.

4 Summary and conclusions

We report the successful application of a total reactive nitrogen (N_r) system for conversion of gas-phase and particle-bound N_r-compounds. The N_r system was tested using laboratory-generated monodisperse aerosol from solutions of $(NH_4)_2SO_4$, NH_4Cl, $NaNO_3$, and $(NH_4)_2C_2O_4$. The particle conversion efficiency of each compound was calculated at each size-selected diameter by the ratio of the concentration measured as N_r to mass concentrations calculated from number concentration and size distribution measurements using a CPC and UHSAS. Overall, the particle conversion efficiency for a selection of N_r-containing aerosols ranged from 93–101% with an overall estimated uncertainty of ~10%. The N_r- particles tested in these experiments span the range of N oxidation states, and therefore we are confident these results extend to other N_r-containing particles. Most catalyst-based N_r systems measure total gas-phase N_r-only, individual N_r-compounds (e.g. NH_3), or ignore the contribution of particulate N_r to total signal completely. However, it is useful to measure the total unspeciated N_r signal, which includes both gases and particles, to improve our understanding of total N-emissions and their deposition, loss, and availability in ecosystems (e.g. McCalley and Sparks, 2009). We have presented a rapid, robust measurement technique that quantitatively measures particle N_r mass that allows for accurately interpreting ambient measurements, and allows improved mass closure of the N-budget to be constructed for the 2016 Fire Sciences Laboratory measurements of wildfire emissions. Future applications of this custom system aim to distinguish gas- and particle-phase nitrogen contributions to total measured N_r signal using upstream filters and denuders.

Additional characterization tests showed the platinum catalyst in the N_r system quantitatively converts both gaseous- and particulate-organic carbon (OC) to CO_2 to within the propagated uncertainties of each detection method (± 10% each). The resulting N_r and C_y signals from each detector are in proportion to the number of carbon and nitrogen atoms in the parent molecule. In order for this to be a reliable total particulate carbon measurement system under ambient conditions, a highly accurate and precise CO_2 measurement system is imperative to measure the signal above ambient CO_2, CO, and CH_4 backgrounds. Alternatively, ambient gas-phase constituents could be effectively eliminated from the sampling matrix. For these reasons, the application of the system is currently limited to calibration of single-component OC- and/or N_r-containing particles.

After establishing efficient conversion of N_r-particles, we experimentally demonstrated that this technique can be used to calibrate aerosol particle mass measurement methods when sampling pure N_r-containing polydisperse aerosol. The N_r equivalent mass measurements of pure atomized polydisperse aerosol showed an agreement of ± 6% with the PILS-ESI/MS measurements of the corresponding anion for the salts $(NH_4)_2SO_4$, NH_4Cl, $NaNO_3$, and NH_4NO_3. There is a clear advantage to calibrating the entire PILS-ESI/MS system altogether as this avoids complications arising from calibrating the ESI/MS and PILS independently. We conclude that the N_r system is an

effective measurement technique that can be used to directly calibrate aerosol mass measurement instruments. With this direct mass calibration method, complications that arise due to optical (e.g. refractive index) and physical properties (e.g. morphologies) in particle number calibration methods are avoided. Additionally, this method is an on-line technique that provides a rapid measurement of particle mass unlike off-line mass measurement methods such as filter analyses. The N_r converter described followed by NO and CO_2 detection is a viable new approach for calibrating aerosol mass instrumentation for both N-containing and organic carbon particles.

Data availability

The data from the laboratory tests are available on request. Data from the 2016 Missoula Fire lab are available here: https://esrl.noaa.gov/csd/groups/csd7/measurements/2016firex/FireLab/DataDownload/index.php?page=/csd/groups/csd7/measurements/2016firex/FireLab/DataDownload/

Author contribution

CES wrote the paper with help from JMR. CES performed the particle calibrations with help from RAW and AK. JMR and YL built the N_r catalyst and performed the tests to verify gas-phase conversion of N_r species. AM advised on operation of the PILS. BW, RKT, and CES designed, constructed, and characterized the ESI interface. VS, RJY, KJZ, CW, and KS made measurements of individual N- species during the FIREX campaign.

Competing interests

The authors declare no competing interests or other conflicts of interest.

Disclaimer

Mention of commercial products is for identification purposes only and does not imply endorsements.

Acknowledgements

This work was supported by NOAA's Climate and Health of the Atmosphere initiatives. C.S. acknowledges support from the National Research Council Research Associateship Program. B. W. was supported by the Kościuszko Foundation Program for Advanced Study, Research and/or Teaching in the United States 2014-2015. A. K. is supported by the Austrian Science Fund FWF's Erwin Schrodinger Fellowship J-3613.The FIREX Fire Lab study was supported in part by the NOAA Climate Office's Atmospheric Chemistry, Carbon Cycle, and Climate program. We thank Dr. Brad Hall for the use of his nitrous oxide standard. We thank S. N. Anthony and the Jarrold group for giving us an ion carpet board for the ESI interface. We thank Matthew Coggon, Abigail Koss, and Joost de Gouw, for their H_3O^+ CIMS data and Steven Brown for his airborne cavity enhanced spectrometer data. We would like to thank Katherine Manfred, Alessandro Franchin, and Charles Brock for their useful discussions.

References

Anthony, S. N., Shinholt, D. L., and Jarrold, M. F.: A simple electrospray interface based on a DC ion carpet, Int. J. Mass Spectrom., 371, 1-7, doi:10.1016/j.ijms.2014.06.007, 2014.

1 Bahreini, R., Ervens, B., Middlebrook, A. M., Warneke, C., de Gouw, J. A., DeCarlo, P. F., Jimenez, J. L., Brock, C.
2 A., Neuman, J. A., Ryerson, T. B., Stark, H., Atlas, E., Brioude, J., Fried, A., Holloway, J. S., Peischl, J., Richter,
3 D., Walega, J., Weibring, P., Wollny, A. G., and Fehsenfeld, F. C.: Organic aerosol formation in urban and
4 industrial plumes near Houston and Dallas, Texas, J. Geophys. Res., 114, D00F16, doi:10.1029/2008JD011493,
5 2009.

6 Bauer, S. E., Koch, D., Unger, N., Metzger, S. M., Shindell, D. T., and Streets, D. G.: Nitrate aerosols today and in
7 2030: a global simulation including aerosols and tropospheric ozone, Atmos. Chem. Phys., 7, 5043-5059,
8 doi:10.5194/acp-7-5043-2007, 2007.

9 Bellouin, N., Rae, J., Jones, A., Johnson, C., Haywood, J., and Boucher, O.: Aerosol forcing in the Climate Model
10 Intercomparison Project (CMIP5) simulations by HadGEM2-ES and the role of ammonium nitrate, J. Geophys.
11 Res., 116, D20206, doi:10.1029/2011JD016074, 2011.

12 Benedict, K. B., Prenni, A. J., Carrico, C. M., Sullivan, A. P., Schichtel, B. A., and Collett Jr., J. L.: Enhanced
13 concentrations of reactive nitrogen species in wildfire smoke, 148, 8-15, doi:10.1016/j.atmosenv.2016.10.030, 2017.

14 Bohren, C. F., and Huffman, D. R.: Absorption and scattering of light by small particles, Wiley, New York, 1983.

15 Breitenbach, L. P. and Shelef, M.: Development of a method for the analysis of NO_2 and NH_3 by NO-measuring
16 instruments, J. Air Pollut. Contr. Assoc., 23, 128-131, doi:10.1080/00022470.1973.10469752, 1973.

17 Burling, I. R., Yokelson, R. J., Griffith, D. W. T., Johnson, T. J., Veres, P., Roberts, J. M., Warneke, C., Urbanski,
18 S. P., Reardon, J., Weise, D. R., Hao, W. M., and de Gouw, J.: Laboratory measurements of trace gas emissions
19 from biomass burning of fuel types from the southeastern and southwestern United States, Atmos. Chem. Phys., 10,
20 11115–11130, doi:10.5194/acp-10-11115-2010, 2010.

21 Cai, Y., Montague, D. C., Mooiweer-Bryan, W., and Deshler, T.: Performance characteristics of the ultra high
22 sensitivity aerosol spectrometer for particles between 55 and 800 nm: Laboratory and field studies, J. Aerosol Sci.,
23 39, 759-769, doi:10.1016/j.jaerosci.2008.04.007, 2008.

24 Canagaratna, M. R., Jayne, J. T., Jimenez, J. L., Allan, J. D., Alfarra, M. R., Zhang, Q., Onasch, T. B., Drewnick, F.,
25 Coe, H., Middlebrook, A., Delia, A., Williams, L. R., Trimborn, A. M., Northway, M. J., DeCarlo, P. F., Kolb, C.
26 E., Davidovits, P. and Worsnop, D. R.: Chemical and microphysical characterization of ambient aerosols with the
27 aerodyne aerosol mass spectrometer, Mass Spectrom. Rev., 26, 185–222, doi:10.1002/mas.20115, 2007.

28 Cape, J. N., Cornell, S. E., Jickells, T. D., and Nemitz, E.: Organic nitrogen in the atmosphere-Where does it come
29 from? A review of sources and methods, Atmos. Res., 102, 30-48, doi:10.1016/j.atmosres.2011.07.009, 2011.

30 Chen, B., T., Fletcher, R., A., and Cheng, Y.,-S.: Calibration of Aerosol Instruments, in Aerosol Measurement:
31 Principles, Techniques, and Applications, Third Edition (eds P. Kulkarni, P. A. Baron and K. Willeke), John Wiley
32 & Sons, Inc., Hoboken, NJ, USA. doi:10.1002/9781118001684.ch21, 2011

1 Collins, D. R., Flagan, R. C., and Seinfeld, J. H.: Improved inversion of scanning DMA Data, Aerosol Sci. Technol.,
2 36:1, 1-9, doi:10.1080/027868202753339032, 2002.

3 Cornell, S. E.: Atmospheric nitrogen deposition: revising the question of the importance of the organic component,
4 Environ. Pollut,. 159, 2214–2222, doi:10.1016/j.envpol.2010.11.014, 2010.

5 DeCarlo, P. F., Slowik, J. G., Worsnop, D. R., Davidovits, P., and Jimenez, J. L.: Particle morphology and density
6 characterization by combined mobility and aerodynamic diameter measurements. Part 1: Theory, Aerosol Sci. Tech.,
7 38, 1185-1205, doi:10.1080/027868290903907, 2004.

8 DeCarlo, P. F., Kimmel, J. R., Trimborn, A., Northway, M. J., Jayne, J. T., Aiken, A. C., Gonin, M., Fuhrer, K.,
9 Horvath, T., Docherty, K. S., Worsnop, D. R., and Jimenez, J. L.: Field-deployable, high resolution, time-of-flight
10 aerosol mass spectrometer, Anal. Chem, 78, 8281-8289, doi:10.1021/ac061249n, 2006.

11 Drewnick, F., Schwab, J. J., Hogrefe, O., Peters, S., Husain, L., Diamnon, D., Weber, R., and Demerjian, K. L.:
12 Intercomparison and evaluation of four semi-continuous $PM_{2.5}$ sulfate instruments, Atmos. Environ., 37, 3335-3350,
13 doi:10.1016/S1352-2310(03)00351-0, 2003.

14 Dunlea, E. J., Herndon, S. C., Nelson, D. D., Volkamer, R. M., San Martini, F., Sheehy, P. M., Zahniser, M. S.,
15 Shorter, J. H., Wormhoudt, J. C., Lamb, B. K., Allwine, E. J., Gaffney, J. S., Marley, N. A., Grutter, M., Marquez,
16 C., Blanco, S., Cardenas, B., Retama, A., Ramos Villegas, C. R., Kolb, C. E., Molina, L. T., and Molina, M. J.:
17 Evaluation of nitrogen dioxide chemiluminescence monitors in a polluted urban environment, Atmos. Chem. Phys.,
18 7, 2691-2704, doi:10.5194/acp-7-2691-2007, 2007.

19 Fahey, D., Eubank, C., Hübler, G., and Fehsenfeld, F.: Evaluation of a catalytic reduction technique for the
20 measurement of total reactive odd-nitrogen NOy in the atmosphere, J. Atmos. Chem., 3, 435−468,
21 doi:10.1007/BF00053871, 1985.

22 Fahey, D. W., Hübler, G., Parrish, D. D., Williams, E. J., Norton, R. B., Ridley, B. A., Singh, H. B., Liu, S. C., and
23 Fehsenfeld, F. C.: Reactive nitrogen species in the troposphere: Measurements of NO, NO_2, HNO_3, particulate
24 nitrate, peroxyacetyl nitrate (PAN), O_3, and total reactive odd nitrogen (NO_y) at Niwot Ridge, Colorado, J. Geophys.
25 Res., 91, 9781-9793, doi:10.1029/JD091iD09p09781, 1986.

26 Farmer, D. K., Matsunaga, A., Docherty, K. S., Surratt, J. D., Seinfeld, J. H., Ziemann, P. J., and Jimenez, J. L.:
27 Response of an aerosol mass spectrometer to organonitrates and organosulfates and implications for atmospheric
28 chemistry, P. Natl. Acade. Sci. USA, 107, 6670–6675, doi:10.1073/pnas.0912340107, 2010.

29 Forster, P., Ramaswamy, V., Artaxo, P., Berntsen, T., Betts, R., Fahey, D. W., Haywood, J., Lean, J., Lowe, D. C.,
30 Myhre, G., Nganga, J., Prinn, R., Raga, G., Schulz, M., and Van Dorland, R.: Changes in Atmospheric Constituents
31 and in Radiative Forcing, in: Climate Change 2007: The Physical Science Basis. Contribution of Working Group I
32 to the Fourth Assessment Report of the Intergovernmental Panel on Climate Change, edited by: Solomon, S., Qin,

D., Manning, M., Chen, Z., Marquis, M., Averyt, K. B., Tignor, M., and Miller, H. L., Cambridge University Press, Cambridge, United Kingdom and New York, NY, USA, 2007.

Fuzzi, S., Baltensperger, U., Carslaw, K., Decesari, S., Denier van der Gon, H., Facchini, M. C., Fowler, D., Koren, I., Langford, B., Lohmann, U., Nemitz, E., Pandis, S., Riipinen, I., Rudich, Y., Schaap, M., Slowik, J. G., Spracklen, D. V., Vignati, E., Wild, M., Williams, M., and Gilardoni, S.: Particulate matter, air quality and climate: lessons learned and future needs, Atmos. Chem. Phys., 15, 8217-8299, doi:10.5194/acp-15-8217-2015, 2015.

Griffith, D. W. T., Mankin, W. G., Coffey, M. T., Ward, D. E., and Riebau, A.: FTIR remote sensing of biomass burning emissions of CO_2, CO, CH_4, CH_{2O}, NO, NO_2, NH_3, and N_2O, in: Global Biomass Burning: Atmospheric, Climatic, and Biospheric Implications, edited by: Levine, J. S., MIT Press, Cambridge, 230–239, 1991.

Hand, J. L., and S. M. Kreidenweis, A new method for retrieving particle refractive index and effective density from aerosol size distribution data, Aerosol Sci. Technol., 36, 1012 – 1026, doi:10.1080/02786820290092276, 2002.

Hardy, J. E. and Knarr, J. J.: Technique for measuring the total concentration of gaseous fixed nitrogen species, J. Air Pollut. Contr. Assoc., 32, 376-379, doi:10.1080/00022470.1982.10465412, 1982.

Hauglustaine, D. A., Balkanski, Y., and Schulz, M.: A global model simulation of present and future nitrate aerosols and their direct radiative forcing of climate, Atmos. Chem. Phys., 14, 11031-11063, doi:10.5194/acp-14-11031-2014, 2014.

Haywood, J., Bush, M., Abel, S., Claxton, B., Coe, H., Crosier, J., Harrison, M., Macpherson, B., Naylor, M., and Osborne, S.: Prediction of visibility and aerosol within the operational Met Office Unified Model II?: Validation of model performance using observational data, Q. J. Roy. Meteorol. Soc., 134, 1817–1832, doi:10.1002/qj.275, 2008.

Horstman, D. W.: A technique for measuring total oxides of nitrogen and ammonia by chemiluminescent detection, Analysis Instr., 93-98, 1982.

Hu, D., Chen, J., Ye, X., and Yang, X.: Hygroscopicity and evaporation of ammonium chloride and ammonium nitrate: Relative humidity and size effects on the growth factor, Atmos. Environ., 45, 2349-2355, doi:10.1016/j.atmosenv.2011.02.024, 2011.

Huffman, J. A., Docherty, K. S., Aiken, A. C., Cubison, M. J., Ulbrich, I. M., DeCarlo, P. F., Sueper, D., Jayne, J. T., Worsnop, D. R., Ziemann, P. J., and Jimenez, J. L.: Chemically-resolved aerosol volatility measurements from two megacity field studies, Atmos. Chem. Phys., 9, 7161-7182, doi:10.5194/acp-9-7161-2009, 2009.

IPCC: Climate Change 2013, The Physical Science Basis, Bern, Switzerland, 2013.

Jayne, J. T., Leard, D. C., Zhan, X., Davidovits, P., Smith, K. A., Kolb, C. E., and Worsnop, D. R.: Development of an aerosol mass spectrometer for size and composition analysis of submicron particles, Aerosol Sci. and Technol., 33:1-2, 49-70, doi: 10.1080/027868200410840, 2000.

Jimenez, J. L., Canagaratna, M. R., Donahue, N. M., Prevot, A. S. H., Zhang, Q., Kroll, J. H., DeCarlo, P. F., Allan, J. D., Coe, H., Ng, N. L., Aiken, A. C., Docherty, K. S., Ulbrich, I. M., Grieshop, A. P., Robinson, A. L., Duplissy, J., Smith, J. D., Wilson, K. R., Lanz, V. A., Hueglin, C., Sun, Y. L., Tian, J., Laaksonen, A., Raatikainen, T., Rautiainen, J., Vaattovaara, P., Ehn, M., Kulmala, M., Tomlinson, J. M., Collins, D. R., Cubison, M. J., Dunlea, E. J., Huffman, J. A., Onasch, T. B., Alfarra, M. R., Williams, P. I., Bower, K., Kondo, Y., Schneider, J., Drewnick, F., Borrmann, S., Weimer, S., Demerjian, K., Salcedo, D., Cottrell, L., Griffin, R., Takami, A., Miyoshi, T., Hatakeyama, S., Shimono, A., Sun, J. Y., Zhang, Y. M., Dzepina, K., Kimmel, J. R., Sueper, D., Jayne, J. T., Herndon, S. C., Trimborn, A. M., Williams, L. R., Wood, E. C., Middlebrook, A. M., Kolb, C. E., Baltensperger, U., and Worsnop, D. R.: Evolution of organic aerosols in the atmosphere, Science, 326, 1525–1529, doi:10.1126/science.1180353, 2009.

Jimenez, J. L., Canagaratna, M. R., Drewnick, F., Allan, J. D., Alfarra, M. R., Middlebrook, A. M., Slowik, J. G., Zhang, Q., Coe, H., Jayne, J. T., and Worsnop, D. R.: Comment on "The effects of molecular weight and thermal decomposition on the sensitivity of a thermal desorption aerosol mass spectrometer", Aerosol Sci. and Technol., 50(9), i-xv, 2016.

Jickells, T., Baker, A., R., Cape, J., N., Cornell, S., E., and Nemitz, E.: The cycling of organic nitrogen through the atmosphere, Philos. Trans. R Soc. Lond. B Biol. Sci., 368, 1621, doi: 10.1098/rstb.2013.0115, 2013.

Kamal, M. S., Razzak, S. A., and Hossain, M. M.: Catalytic oxidation of volatile organic compounds (VOCs) - A review, Atmos. Environ., 140, 117-134, doi:10.1016/j.atmosenv.2016.05.031, 2016

Kiyoura, R. and Urano, K.: Mechanism, kinetics and equilibrium of thermal decomposition of ammonium sulfate, Ind. Eng. Chem. Process Des. Develop., 9, 489-494, doi:10.1021/i260036a001, 1970.

Knutson, E. O. and Whitby, K. T.: Aerosol classification by electric mobility: Apparatus, theory, and applications, J. Aerosol Sci., 6, 443–451, doi:10.1016/0021-8502(75)90060-9, 1975.

Koss, A. R., Sekimoto, K., Gilman, J. B., Selimovic, V., Coggon, M. M., Zarzana, K. J., Yuan, B., Lerner, B. M., Brown, S. S., Jimenez, J. L., Krechmer, J., Roberts, J. M., Warneke, C., Yokelson, R. J., and de Gouw, J.: Non-methane organic gas emissions from biomass burning: identification, quantification, and emission factors from PTR-ToF during the FIREX 2016 laboratory experiment, Atmos. Chem. Phys. Discuss., https://doi.org/10.5194/acp-2017-924, in review, 2017.

Kostiainen, R., and Kauppila, T. J.: Effect of eluent on the ionization process in liquid chromatography-mass spectrometry, J. Chrom. A., 1216(4), 685-699, doi:10.1016/j.chroma.2008.08.095, 2009.

Kuhlbusch, T. A., Lobert, J. M., Crutzen, P. J., and Warneck, P.: Molecular nitrogen emissions from denitrifcation during biomass burning, Nature, 351, 135-137, doi:10.1038/351135a0, 1991.

Kupc, A., Williamson, C., Wagner, N. L., Richardson, M., and Brock, C. A.: Modification, Calibration, and Performance of the Ultra-High Sensitivity Aerosol Spectrometer for Particle Size Distribution and Volatility Measurements During the Atmospheric Tomography (ATom) Airborne Campaign, Atmos. Meas. Tech. Discuss., https://doi.org/10.5194/amt-2017-293, in review, 2017.

Lee, B. H., Mohr, C., Lopez-Hilfiker, F. D., Lutz, A., Hallquist, M., Lee, L., Romer, P., Cohen, R. C., Iyer, S., Kurten, T., Hu, W. W., Day, D. A., Campuzano-Jost, P., Jimenez, J. L., Xu, L., Ng, N. L., Guo, H., Weber, R. J., Wild, R. J., Brown, S. S., Koss, A., de Gouw, J., Olson, K., Goldstein, A. H., Seco, R., Kim, S., McAvey, K. M., Shepson, P. B., Starn, T., Baumann, K., Edgerton, E., Liu, J., Shilling, J. E., Miller, D. O., Brune, W. H., Schobesberger, S., D'Ambro, E. L., and Thornton, J. A.: Highly functionalized organic nitrates in the Southeast U.S.: contribution to secondary organic aerosol and reactive nitrogen budgets, Proc. Natl. Acad. Sci., 113, 1516–1521, doi:10.1073/pnas.1508108113, 2016.

Li, J., Wang, W-C., Liao, H., and Chang, W.: Past and future direct radiative forcing of nitrate aerosol in East Asia, Theor. Appl. Climatol., 121, 445-458, doi: 10.1007/s00704-014-1249-1, 2015.

Liao, H., Adams, P. J., Chung, S. H., Seinfeld, J. H., Mickley, L. J., and Jacob, D. J.: Interactions between tropospheric chemistry and aerosols in a unified general circulation model, J. Geophys. Res., 108(D1), 4001, doi:10.1029/2001JD001260, 2003.

Lin, M., Walker, J., Geron, C., and Khlystov, A.: Organic nitrogen in PM2.5 aerosol at a forest site in the Southeast US, Atmos. Chem. Phys., 10, 2145-2157, doi:10.5194/acp-10-2145-2010, 2010.

Liu, Y., and Daum, P. H.: The effect of refractive index on size distributions and light scattering coefficients derived from optical particle counters, J. Aerosol Sci., 31, 945-957, doi:10.1016/S0021-8502(99)00573-X, 2000.

Liu, B. Y. H. and Lee, K.W.: An aerosol generator of high stability, Am. Ind. Hyg. Assoc. J., 36, 861–865, doi:10.1080/0002889758507357, 1975.

Lobert, J. M., Scharffe, D. H., Hao, W. M., and Crutzen, P. J.: Importance of biomass burning in the atmospheric budgets of nitrogen-containing gases, Nature, 346, 552-554, doi:10.1038/346552a0, 1990.

Lobert, J. M., Scharffe, D. H., Hao, W.-M., Kuhlbusch, T. A., Seuwen, R., Warneck, P., and Crutzen, P. J.: Experimental evaluation of biomass burning emissions: Nitrogen and carbon containing compounds. In: Global Biomass Burning: Atmospheric, Climatic, and Biospheric Implications, Levine, J. S. (Ed.), The MIT Press, Cambridge, MA, 1991.

Ma, Y.: Developments and Improvements to the Particle-Into-Liquid Sampler (PILS) and its Application to Asian Outflow Studies, Ph.D. Dissertation, Georgia Institute of Technology, Atlanta, GA, 2004.

Maris, C., Chung, M. Y., Lueb, R., Krischke, U., Meller, R., Fox, M. J., and Paulson, S. E.: Development of instrumentation for simultaneous analysis of total non-methane organic carbon and volatile organic compounds in ambient air, Atmos. Environ., 37, S149-S158, doi:10.1016/S1352-2310(03)00387-X, 2003.

Marx, O., Brümmer, C., Ammann, C., Wolff, V., and Freibauer, A.: TRANC – a novel fast-response converter to measure total reactive atmospheric nitrogen, Atmos. Meas. Tech., 5, 1045-1057, doi:10.5194/amt-5-1045-2012, 2012.

McCalley, C. K. and Sparks, J. P.: Abiotic gas formation drives nitrogen loss from a desert ecosystem, Science, 326, 837–840, doi:10.1126/science.1178984, 2009.

McMeeking, G. R., Kreidenweis, S. M., Baker, S., Carrico, C. M., Chow, J. C., Collet Jr., J. L., Hao, W. M., Holden, A. S., Kirchstetter, T. W., Malm, W. C., Moosmüller, H., Sullivan, A. P., and Wold, C. E.: Emissions of trace gases and aerosols during the open combustion of biomass in the laboratory, J. Geophys. Res., 114, D19210, doi:10.1029/2009JD011836, 2009.

McMurry, P. H.: A review of atmospheric aerosol measurements, Atmos. Environ., 34, 1959-1999, doi.org/10.1016/S1352-2310(99)00455-0, 2000.

Min, K.-E., Washenfelder, R. A., Dubé, W. P., Langford, A. O., Edwards, P. M., Zarzana, K. J., Stutz, J., Lu, K., Rohrer, F., Zhang, Y., and Brown, S. S.: A broadband cavity enhanced absorption spectrometer for aircraft measurements of glyoxal, methylglyoxal, nitrous acid, nitrogen dioxide, and water vapor, Atmos. Meas. Tech., 9, 423-440, https://doi.org/10.5194/amt-9-423-2016, 2016.

Murphy, D. M.: The effects of molecular weight and thermal decomposition on the sensitivity of a thermal desorption aerosol mass spectrometer, Aerosol Sci. and Technol., 50(2), 118-125, doi:10.1080/02786826.2015.1136403, 2016a.

Murphy, D. M.: Reply to Comment on the effects of molecular weight and thermal decomposition on the sensitivity of a thermal desorption aerosol mass spectrometer", by Jimenez et al., Aerosol Sci. and Technol., 50, 1277-1283, 2016b.

Neff, J. C., Holland, E. A., Dentener, F. J., McDowell, W. H., and Russell, K. M.: The origin, composition and rates of organic nitrogen deposition: A missing piece of the nitrogen cycle?, Biogeochemistry, 57, 99–136, 2002.

Neuman, J. A., Huey, L. G., Ryerson, T. B., and Fahey, D. W.: Study of inlet materials for sampling atmospheric nitric acid, Environ. Sci. Technol., 33(7), 1133-1136, doi: 10.1021/es980767f, 1999.

Neuman, J. A., Ryerson, T. B., Huey, L. G., Jakoubek, R., Nowak, J. B., Simons, G., and Fehsenfeld, F. C.: Calibration and evaluation of nitric acid and ammonia permeation tubes by UV optical absorption, Environ. Sci. Technol., 37, 2975-2981, doi:10.1021/es026422l, 2003.

NIST Chemical Kinetics Database, Standard Reference Database 17, Version 7.0 Web Version, accessed September 18, 2017.

Orsini, D. A., Ma, Y., Sullivan, A., Sierau, B., Baumann, K., and Weber, R. J.: Refinements to the particle-into-liquid sampler (PILS) for ground and airborne measurements of water-soluble aerosol composition, Atmos. Environ., 37, 1243–1259, doi:10.1016/S1352-2310(02)01015-4, 2003.

Park, R. S., Lee, S., Shin, S.-K., and Song, C. H.: Contribution of ammonium nitrate to aerosol optical depth and direct radiative forcing by aerosols over East Asia, Atmos. Chem. Phys., 14, 2185-2201, doi:10.5194/acp-14-2185-2014, 2014.

Parrish, D. D. and Fehsenfeld, F. C.: Methods for gas-phase measurements of ozone, ozone precursors and aerosol precursors, Atmos. Environ., 34, 1921–1957, doi: 10.1016/S1352-2310(99)00454-9, 2000.

Pöschl, U.: Atmospheric aerosols: Composition, transformation, climate and health effects, Angew. Chem. Int. Ed, 44, 7520-7540, doi:10.1002/anie.200501122, 2005.

Prenni, A. J., Levin, E. J. T., Benedict, K. B., Sullivan, A. P., Schurman, M. I., Gebhart, K. A., Day, D. E., Carrico, C. M., Malm, W. C., Schichtel, B. A., Collet Jr., J. L., and Kreidenweis, S. M.: Gas-phase reactive nitrogen near Grand Teton National Park: Impacts of transport, anthropogenic emissions, and biomass burning, Atmos. Environ., 89, 749-756, doi:10.1016/j.atmosenv.2014.03.017, 2014.

Roberts, J. M., Bertman, S. B., Jobson, T., Niki, H., and Tanner, R.: Measurement of total nonmethane organic carbon (Cy): development and application at Chebogue Point, Nova Scotia, during the 1993 North Atlantic Regional Experiment campaign, J. Geophys. Res.-Atmos., 103, 13581–13592, doi:10.1029/97JD02240, 1998.

Roberts, J. M., Veres, P., Warneke, C., Neuman, J. A., Washenfelder, R. A., Brown, S. S., Baasandorj, M., Burkholder, J. B., Burling, I. R., Johnson, T. J., Yokelson, R. J., and de Gouw, J.: Measurement of HONO, HNCO, and other inorganic acids by negative-ion proton-transfer chemical-ionization mass spectrometry (NI-PT-CIMS): application to biomass burning emissions, Atmos. Meas. Tech., 3, 981-990, doi:10.5194/amt-3-981-2010, 2010.

Rosenberg, P. D., Dean, A. R., Williams, P. I., Dorsey, J. R., Minikin, A., Pickering, M. A., and Petzold, A.: Particle sizing calibration with refractive index correction for light scattering optical particle counters and impacts upon PCASP and CDP data collected during the Fennec campaign, Atmos. Meas. Tech., 5, 1147-1163, doi:10.5194/amt-5-1147-2012, 2012.

Russell, L. M., Flagan, R. C., and Seinfeld, J. H.: Asymmetric instrument response resulting from mixing effects in accelerated DMA-CPC measurements, Aerosol Sci. Technol., 23:4, 491-509, doi: 10.1080/02786829508965332, 1995.

Saylor, R. D., Edgerton, E. S., Hartsell, B. E., Baumann, K., and Hansen, D. A.: Continuous gaseous and total ammonia measurements from the southeastern aerosol research and characterization (SEARCH) study, Atmos. Environ., 44, 4994-5004, doi:10.1016/j.atmosenv.2010.07.055, 2010.

Schwab, J. J., Li, Y., Bae, M.-S., Demerjian, K. L., Hou, J., Zhou, X., Jensen, B., and Pryor, S.: A laboratory intercomparision of real-time gaseous ammonia measurement methods, Environ. Sci. Technol., 41, 8412-8419, doi:10.1021/es070354r, 2007.

Schwartz, A., Holbrook, L. L., and Wise, H.: Catalytic oxidation studies with platinum and palladium, J. Catalysis, 21, 199-207, doi: 10.1016/0021-9517(71)90138-2, 1971.

Selimovic, V., Yokelson, R. J., Warneke, C., Roberts, J. M., de Gouw, J., Reardon, J., and Griffith, D. W. T.: Aerosol optical properties and trace gas emissions by PAX and OP-FTIR for laboratory-simulated western US wildfires during FIREX, Atmos. Chem. Phys. Discuss., https://doi.org/10.5194/acp-2017-859, in review, 2017.

Sorooshian, A., Brechtel, F. J., Ma, Y., Weber, R. J., Corless, A., Flagan, R. C., and Seinfeld, J. H.: Modeling and characterization of a Particle-into-Liquid Sampler (PILS), Aerosol Sci. Tech., 40,396–409, doi:10.1080/02786820600632282, 2006.

Stockwell, C. E., Yokelson, R. J., Kreidenweis, S. M., Robinson, A. L., DeMott, P. J., Sullivan, R. C., Reardon, J., Ryan, K. C., Griffith, D. W. T., and Stevens, L.: Trace gas emissions from combustion of peat, crop residue, domestic biofuels, grasses, and other fuels: configuration and Fourier transform infrared (FTIR) component of the fourth Fire Lab at Missoula Experiment (FLAME-4), Atmos. Chem. Phys., 14, 9727-9754, doi:10.5194/acp-14-9727-2014, 2014.

Stockwell, C. E., Veres, P. R., Williams, J., and Yokelson, R. J.: Characterization of biomass burning emissions from cooking fires, peat, crop residue, and other fuels with high-resolution proton-transfer-reaction time-of-flight mass spectrometry, Atmos. Chem. Phys., 15, 845-865, doi:10.5194/acp-15-845-2015, 2015.

Stolzenburg, M.: An Ultrafine Aerosol Size Distribution Measuring System, PhD. thesis, Mechanical Engineering Department, University of Minnesota, USA, 1988.

Stolzenburg, M. R., and McMurry, P. H.: An ultrafine aerosol condensation nucleus counter, Aerosol Sci. Technol., 14(1), 48-65, doi:10.1080/02786829108959470, 1991.

Takegawa, N., Miyazaki, Y., Kondo, Y., Komazaki, Y., Miyakawa, T., Jimenez, J. L., Jayne, J. T., Worsnop, D. R., Allan, J. D., and Weber, R. J.: Characterization of an Aerodyne aerosol mass spectrometer (AMS): Intercomparison with other aerosol instruments, Aerosol Sci. Technol., 39 (8), 760-770, doi:10.1080/02786820500243404, 2005.

Tang, K., Page, J. S., and Smith, R. D.: Charge competition and the linear dynamic range of detection in electrospray ionization mass spectrometry, J. Am. Soc. Mass Spectrom., 15, 1416-1423, doi:10.1016/j.jasms.2004.04.034, 2004.

1 Usherenko, L. N., Fialko, M. B., Kumok, V. N., and Skorik, A. I.: Mechanism and kinetics of thermal-
2 decomposition of ammonium oxalate, J. Appl. Chem. USSR, 61, 1559-1563, 1988.

3 Valentour, J. C., Aggarwal, V., and Sunshine, I.: Sensitive gas chromatographic determination of cyanide, Anal.
4 Chem., 46 (7), 924-925, doi:10.1021/ac60343a048, 1974.

5 Veres, P.V., Roberts, J. M., Warneke, C., and deGouw, J.: Development of negative-ion proton-transfer chemical-
6 ionization mass spectrometry (NI-PT-CIMS) for the measurement of gas-phase organic acids in the atmosphere, Int.
7 J. Mass Spectrom., 274(1–3), 48–55, doi:10.1016/j.ijms.2008.04.032, 2008.

8 Veres, P., Gilman, J. B., Roberts, J. M., Kuster, W. C., Warneke, C., Burling, I. R., and de Gouw, J.: Development
9 and validation of a portable gas phase standard generation and calibration system for volatile organic compounds,
10 Atmos. Meas. Tech., 3, 683-691, doi:10.5194/amt-3-683-2010, 2010.

11 Vieno, M., Heal, M. R., Twigg, M. M., MacKenzie, I. A., Braban, C. F., Lingard, J. J. N. Ritchie, S., Beck, R. C.,
12 A., M., Ots, R., DiMarco, C. F., Nemitz, E., Sutton, M. A., and Reis, S.: The UK particulate matter air pollution
13 episode of March-April 2014: more than Saharan dust., Environ. Res. Lett., doi:10.1088/1748-9326/11/4/044004,
14 2016.

15 Wang, S. C., and Flagan, R. C.: Scanning electrical mobility spectrometer, Aerosol Sci. Technol., 13, 230-240,
16 doi:10.1080/02786829008959441, 1990.

17 Weber, R. J., Orsini, D., Daun, Y., Lee, Y. N., Klotz, P. J., and Brechtel, F. J.: A Particle-Into-Liquid Collector for
18 Rapid Measurement of Aerosol Bulk Chemical Composition, Aerosol Sci. Technol. 35, 718–727,
19 doi:10.1080/02786820152546761, 2001.

20 Wiedensohler, A.: An approximation of the bipolar charge distribution for particles in the sub-micron size range, J.
21 Aerosol Sci., 19, 387–389, doi:10.1016/0021-8502(88)90278-9, 1988.

22 Williams, E. J., Baumann, K., Roberts, J. M., Bertman, S. B., Norton, R. B., Fehsenfeld, F. C., Springston, S. R.,
23 Nunnermacker, L. J., Newman, L., Olszyna, K., Meagher, J., Hartsell, B., Edgerton, E., Pearson, J. R., and Rodgers,
24 M. O.: Intercomparison of ground-based NOy measurement techniques, J. Geophys. Res.-Atmos., 103, 22261-
25 22280, doi:10.1029/98JD00074, 1998.

26 Winer, A. M., Peters, J. W., Smith, J. P., and Pitts, J. N.: Response of commercial chemiluminescent nitric oxide-
27 nitrogen dioxide analyzers to other nitrogen-containing compounds, Environ. Sci. Technol., 8, 1118-1121,
28 doi:10.1021/es60098a004, 1974.

29 Womack, C. C., Neuman, J. A., Veres, P. R., Eilerman, S. J., Brock, C. A., Decker, Z. C. J., Zarzana, K. J., Dube,
30 W. P., Wild, R. J., Wooldridge, P. J., Cohen, R. C., and Brown, S. S.: Evaluation of the accuracy of thermal
31 dissociation CRDS and LIF techniques for atmospheric measurement of reactive nitrogen species, Atmos. Meas.
32 Tech., 10, 1911-1926, doi:10.5194/amt-10-1911-2017, 2017.

1 Xu, L. and Penner, J. E.: Global simulations of nitrate and ammonium aerosols and their radiative effects, Atmos.
2 Chem. Phys., 12, 9479-9504, doi:10.5194/acp-12-9479-2012, 2012.

3 Yokelson, R. J., Christian, T. J., Bertschi, I. T., and Hao, W. M.: Evaluation of adsorption effects on measurements
4 of ammonia, acetic acid, and methanol, J. Geophys. Res., 108, 4649, doi:10.1029/2003JD003549, 2003.

Atmos. Meas. Tech. Discuss., https://doi.org/10.5194/amt-2017-419
Manuscript under review for journal Atmos. Meas. Tech.
Discussion started: 2 January 2018

Atmospheric Measurement Techniques Discussions

1 **Figures**

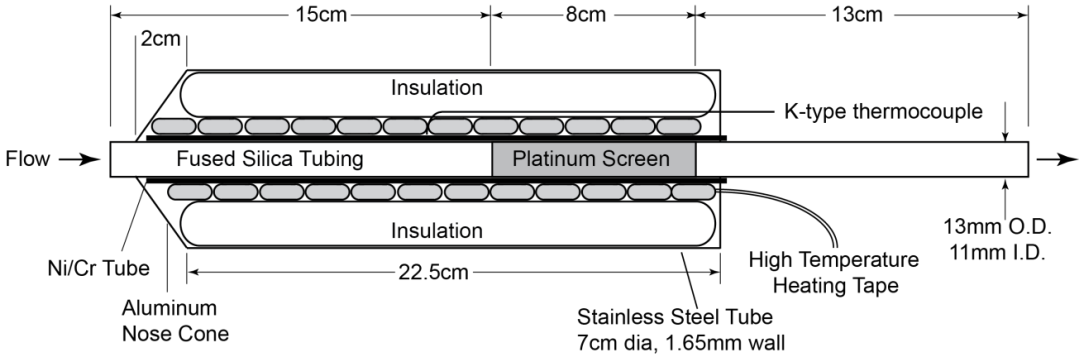

2

3 **Figure 1.** Diagram of the custom-built platinum catalyst system for the total reactive nitrogen instrument (N_r) operated
4 at 750°C. The outlet flow is followed by a molybdenum oxide catalyst before the commercial NO-O_3
5 chemiluminescent instrument.

Atmos. Meas. Tech. Discuss., https://doi.org/10.5194/amt-2017-419
Manuscript under review for journal Atmos. Meas. Tech.
Discussion started: 2 January 2018

Atmospheric Measurement Techniques Discussions

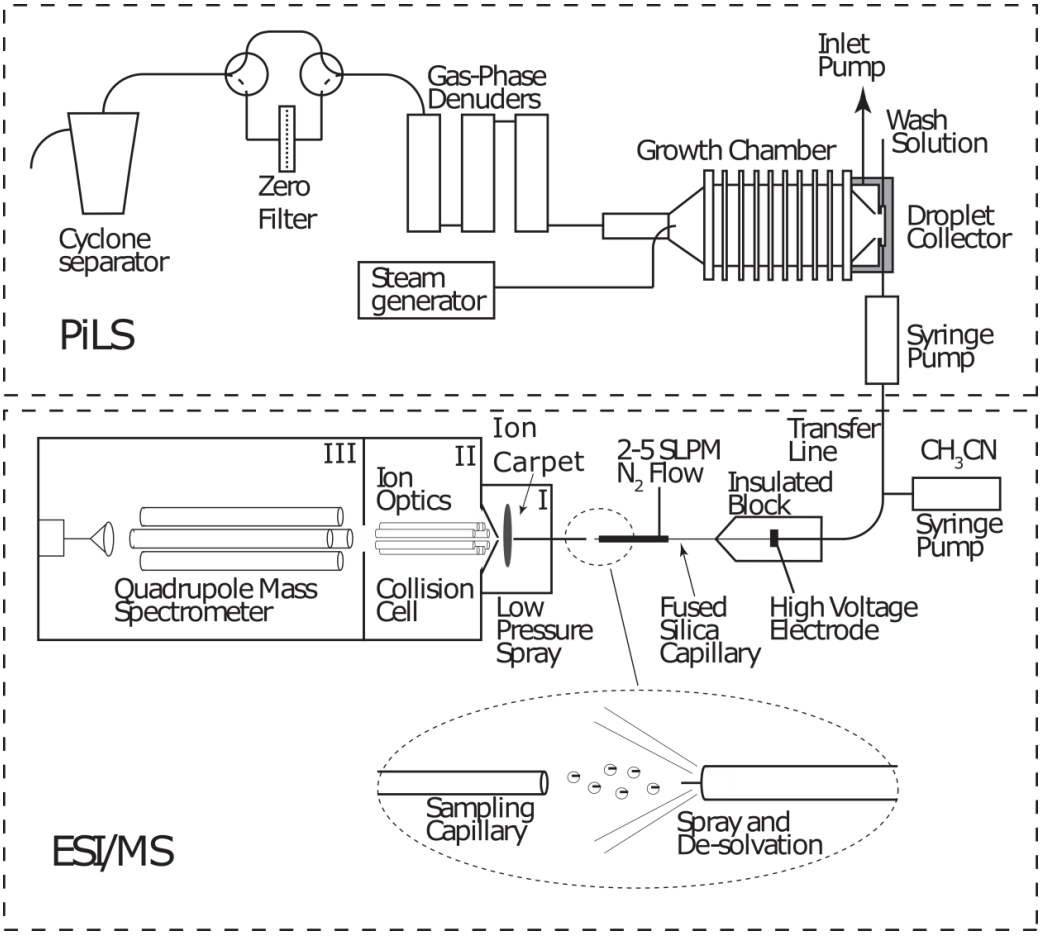

Figure 2. Schematic of a particle-into-liquid sampler (PILS; Sorooshian et al., 2006) interfaced to an electrospray ionization (ESI) source of a quadrupole mass spectrometer (MS) for continuous measurement of water soluble components of atmospheric particles.

Atmos. Meas. Tech. Discuss., https://doi.org/10.5194/amt-2017-419
Manuscript under review for journal Atmos. Meas. Tech.
Discussion started: 2 January 2018

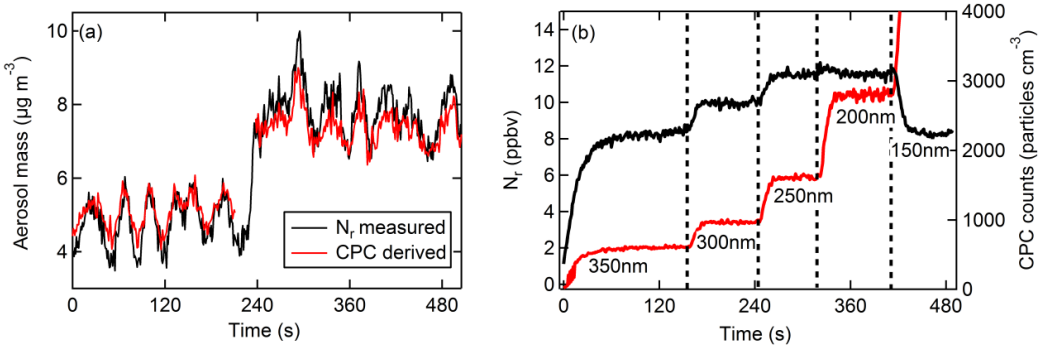

Figure 3. The signal resulting from particles only. (a) Real-time N_r (black) measured and CPC (red) derived aerosol mass concentrations (µg m^{-3}) from an atomized solution of $NaNO_3$. (b) Time response of the N_r signal (ppbv) shown in black (left axis), and the CPC signal (particles cm^{-3}), shown in red (right axis), as particle sizes of $(NH_4)_2SO_4$ are selectively changed. The dashed vertical lines and labels indicate the singly-charged particle diameter selected with the DMA.

Atmos. Meas. Tech. Discuss., https://doi.org/10.5194/amt-2017-419
Manuscript under review for journal Atmos. Meas. Tech.
Discussion started: 2 January 2018

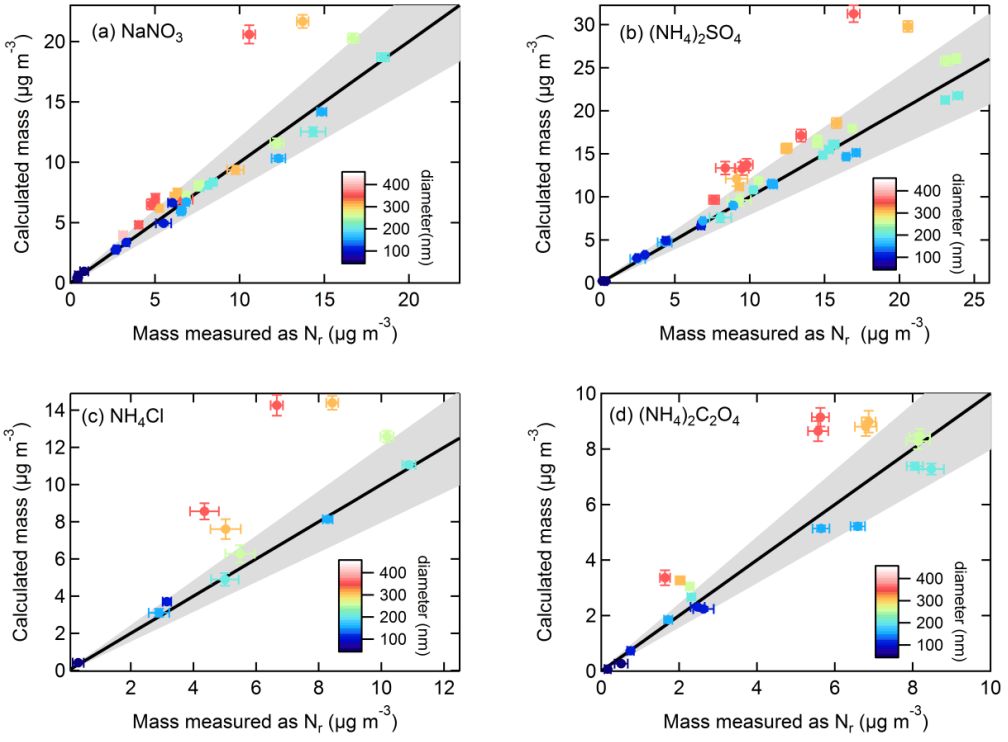

Figure 4. Calculated mass from particles size-selected by the DMA and corrected for multiply charged particles using SMPS-derived size distributions compared to aerosol mass concentrations (µg m^{-3}) measured as N_r for (a) $NaNO_3$, (b) $(NH_4)_2SO_4$, (c) NH_4Cl, and (d) $(NH_4)_2C_2O_4$. The particle size is designated by the color plot (error bars indicate ±1 stdev) and the 1:1 line is shown in black with 20% error indicated by the grey shading.

Atmos. Meas. Tech. Discuss., https://doi.org/10.5194/amt-2017-419
Manuscript under review for journal Atmos. Meas. Tech.
Discussion started: 2 January 2018

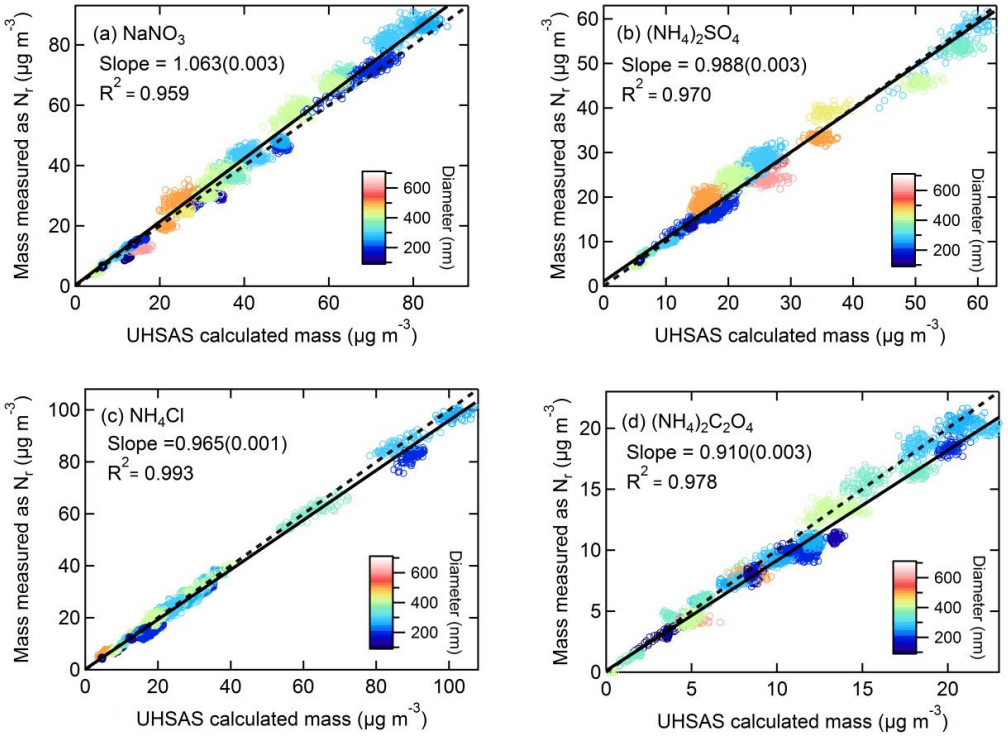

Figure 5. Correlation plots of mass concentrations measured as N_r for (a) $NaNO_3$, (b) $(NH_4)_2SO_4$, (c) NH_4Cl, and (d) $(NH_4)_2C_2O_4$) versus mass concentrations calculated using CPC number concentrations with UHSAS size distributions. Particle sizes (nm) are indicated by the color plot and the 1:1 line is shown in dashed black. The solid lines are orthogonal distance regression fits. The slope (uncertainty) and R^2 is shown.

Atmos. Meas. Tech. Discuss., https://doi.org/10.5194/amt-2017-419
Manuscript under review for journal Atmos. Meas. Tech.
Discussion started: 2 January 2018

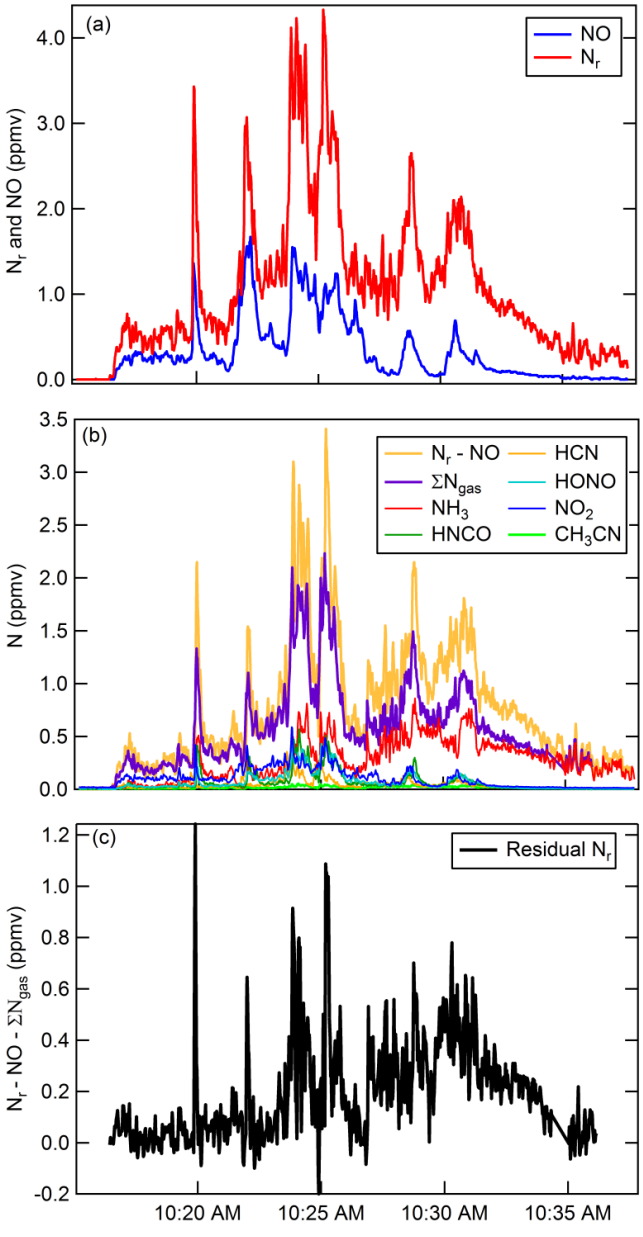

Figure 6. Timeseries for Fire Sciences Lab 2016 measurements of emissions from a subalpine fir canopy sample (Fire 047). (a) Total reactive nitrogen (N_r, red) and nitric oxide (NO, blue) measurements. (b) Comparison of the difference (N_r-NO, gold) with the sum of the measured gas phase N_r-species (purple). The sum of individually measured gas-phase species in order of abundance include: NH_3, HNCO, HCN, HONO, NO_2, CH_3NO_2, and 40 minor organic nitrogen species. NO_2 and HONO were measured by a broadband cavity enhanced extinction spectrometer, HCN and NH_3 were measured by FTIR, and all remaining organic species were measured by H_3O^+ CIMS. (c) Residual N_r in ppmv.

Atmos. Meas. Tech. Discuss., https://doi.org/10.5194/amt-2017-419
Manuscript under review for journal Atmos. Meas. Tech.
Discussion started: 2 January 2018

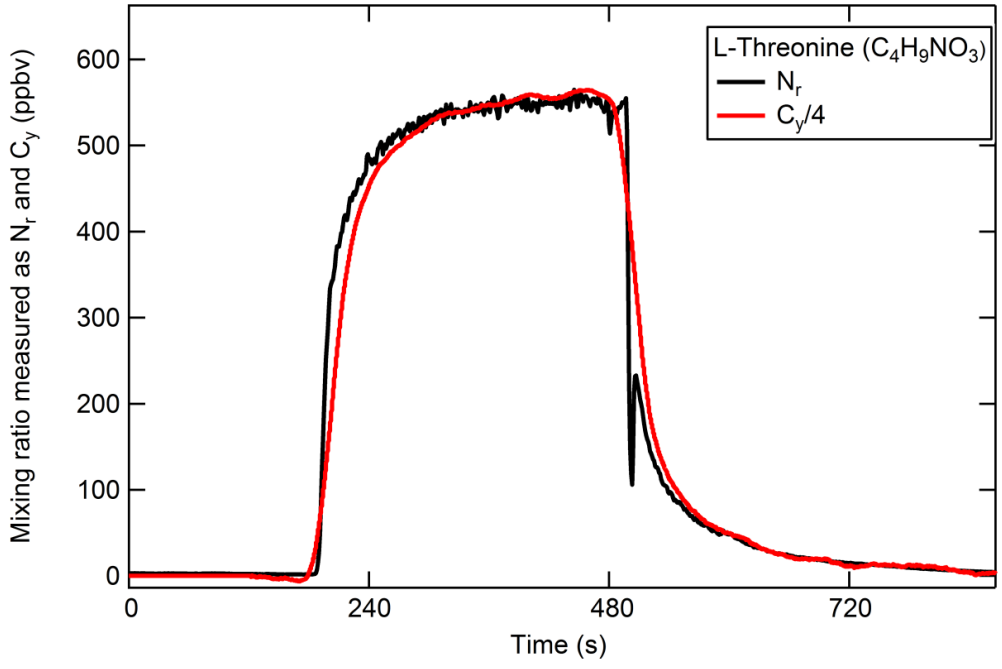

Figure 7. An example of the quantitative conversion of atomized polydisperse threonine ($C_4H_9NO_3$) to NO and CO_2 measured by NO-O_3 chemiluminescence and a LICOR-6251, respectively. The measured total C_y (red) is divided by the number of C atoms in threonine (4).

Atmos. Meas. Tech. Discuss., https://doi.org/10.5194/amt-2017-419
Manuscript under review for journal Atmos. Meas. Tech.
Discussion started: 2 January 2018

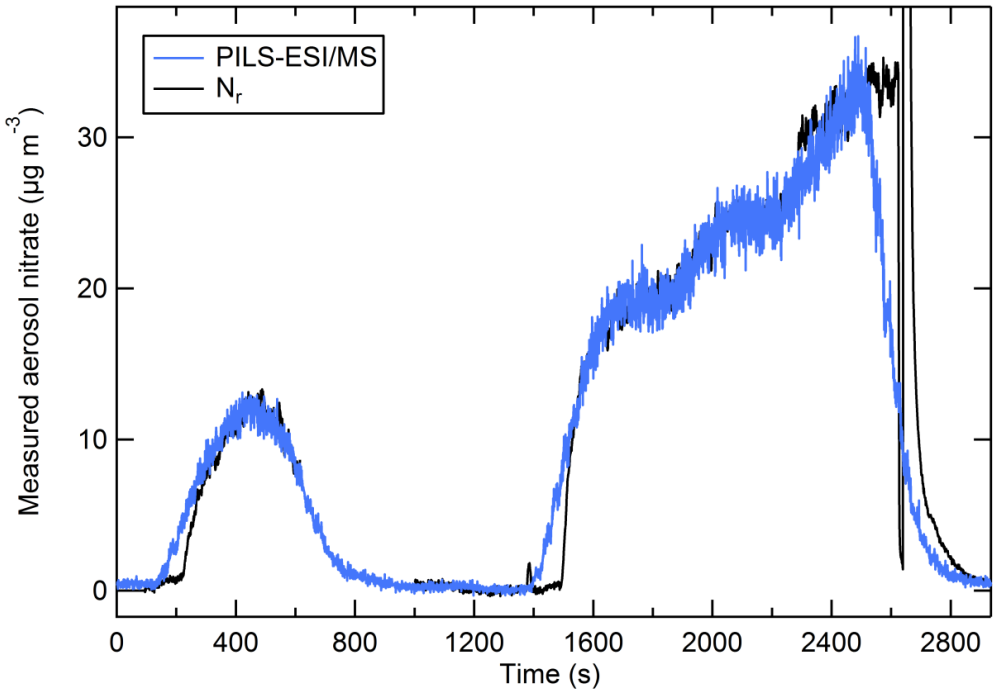

Figure 8. The PILS-ESI/MS measured aerosol nitrate mass (blue) and the nitrate measured as N_r (black) (µg m^{-3}) for an atomized solution of $NaNO_3$ (polydisperse). The PILS-ESI/MS trace is shifted to account for the delayed response and the instrument time constant.

Atmos. Meas. Tech. Discuss., https://doi.org/10.5194/amt-2017-419
Manuscript under review for journal Atmos. Meas. Tech.
Discussion started: 2 January 2018

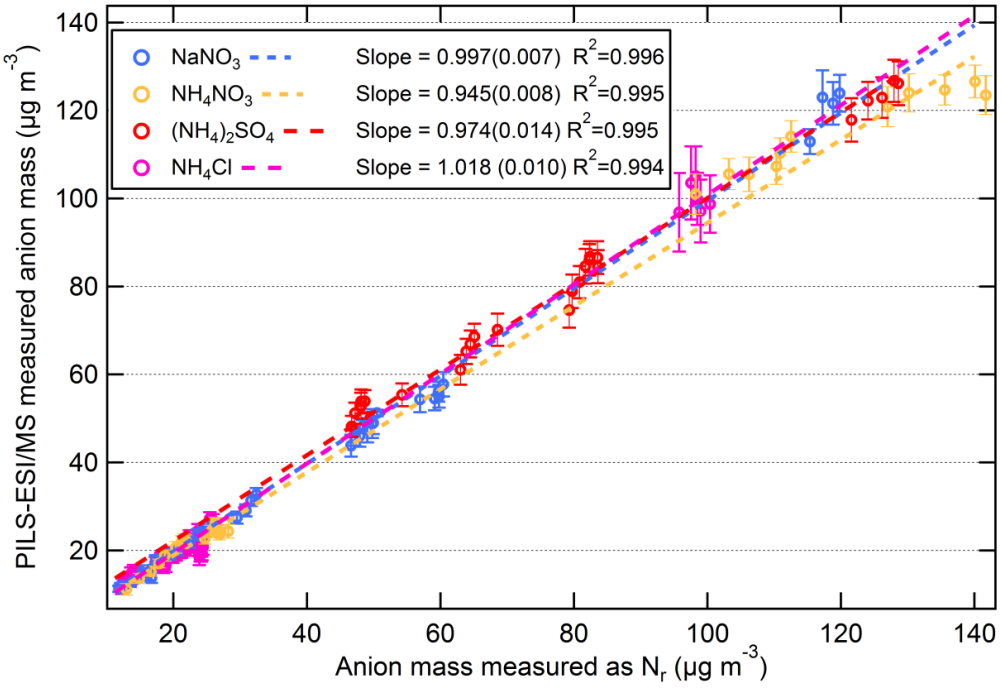

Figure 9. Scatter plots of PILS-ESI/MS measured versus equivalent anion mass measured as N_r for salts $NaNO_3$ (blue), NH_4NO_3 (gold), $(NH_4)_2SO_4$ (red), and NH_4Cl (magenta). The data are 60 s averages and only include times when the atomized aerosol output was relatively constant (i.e. not when concentrations were rising/falling). The slope (1σ) and R^2 is shown.

Atmos. Meas. Tech. Discuss., https://doi.org/10.5194/amt-2017-419
Manuscript under review for journal Atmos. Meas. Tech.
Discussion started: 2 January 2018

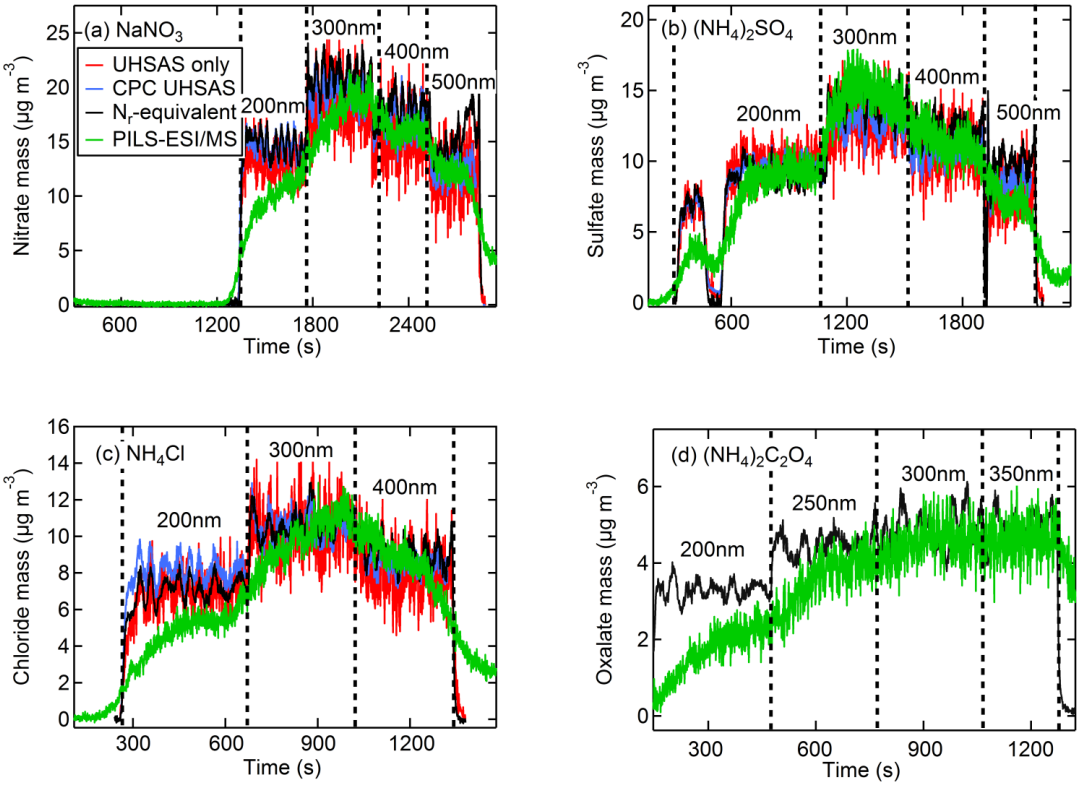

Figure 10. The N_r (black) measured, CPC number with UHSAS size (blue) calculated, UHSAS number and size (red) calculated, and PILS-ESI/MS(green) measured aerosol concentrations (µg m^{-3}) for anions of DMA size selected aerosol for salts of (a) $NaNO_3$, (b) $(NH_4)_2SO_4$, (c) NH_4Cl, and (d) $(NH_4)_2C_2O_4$. The PILS-ESI/MS traces were shifted in time several minutes early to account for the delayed instrument response time.

Atmos. Meas. Tech. Discuss., https://doi.org/10.5194/amt-2017-419
Manuscript under review for journal Atmos. Meas. Tech.
Discussion started: 2 January 2018

Atmospheric Measurement Techniques Discussions

Tables

Table 1. Conversion efficiencies of N_r compounds by the Pt/MoOx catalyst system

Compound	Conversion efficiency (%)	Calibration method	Reference
Nitrogen Dioxide, NO_2	99 ± 2	Titration of NO standard by O_3	Williams et al., 1998
Ammonia, NH_3	105-110 ± 15	Permeation tube or gas mixture, UV absorbance at 184.9nm	Neuman et al., 2003
Hydrogen cyanide, HCN	101-102 ± 10	Gravimetric gas mixture	GASCO, Oldsmar, FL.
Cyanogen chloride, ClCN	98 ± 10	Conversion of HCN standard with Chloramine-T	Valentour et al., 1974
Isocyanic Acid, HNCO	100 ± 25	Decomposition of the trimer, FTIR	Roberts et al., 2010
Nitrobenzene, $C_6H_5NO_2$	95 ± 15	Liquid calibration unit, liquid flow and gravimetric concentration	Ionicon, Innsbruck, Austria
Triethyl amine, $(C_2H_5)_3N$	95 ± 15	Liquid calibration unit, liquid flow and gravimetric concentration	Ionicon, Innsbruck, Austria

Atmos. Meas. Tech. Discuss., https://doi.org/10.5194/amt-2017-419
Manuscript under review for journal Atmos. Meas. Tech.
Discussion started: 2 January 2018

Atmospheric Measurement Techniques Discussions

Table 2. Particle conversion efficiencies (%) with uncertainties (one standard deviation) in parentheses. The sizing accuracy is ~± 2.5% using NIST-traceable PSLs for 150 –500 nm spheres as our calibration standard.

Diameter (nm)	$NaNO_3$	$(NH_4)_2SO_4$	NH_4Cl	$(NH_4)_2C_2O_4$
100	88.4(18.3)	100.6(3.0)	89.2(5.9)	91.0(3.5)
150	94.0(10.9)	96.5(2.5)	93.4(4.7)	89.0(6.6)
200	98.6(4.0)	98.8(4.8)	93.6(4.2)	90.2(5.1)
250	101(3)	100(3)	98.3(3.7)	94.7(5.6)
300	104(6)	102(9)	101(3)	97.0(6.2)
350	102(6)	101(9)	98.5(5.2)	101(13)
400	103(8)	100(8)	100(6)	94.7(7.4)
450	95.1(4.5)	110(4)	103(6)	-
500	103(15)	109(17)	124(11)	96.3(7.6)
600	83.2(8.7)	91.9(5.5)	-	82.5(8.4)
Average	97.3(7.1)	101(5)	100(10)	92.9(5.4)